AERODYNAMIC ANALYSIS OF PIVOTLESS TILTING PAD GAS JOURNAL BEARING

A Thesis Submitted in Partial Fulfillment of the Requirements for the

Award of the Degree of

Master of Technology
In
Mechanical Engineering

(Machine Design & Analysis*)*

By

Pravajyoti Patra

Roll No.213ME1386

Under the Supervision of

Prof. Suraj Kumar Behera

NATIONAL INSTITUTE OF TECHNOLOGY ROURKELA

राष्ट्रीय प्रौधोगिकी संस्थान राउरकेऱा

ROURKELA 769008
ODISHA, INDIA
May 2015

National Institute of Technology Rourkela

Certificate

This is to certify that the thesis entitled, "**Aerodynamic Analysis of Pivotless Tilting Pad Gas Journal Bearing**" submitted by Mr**. Pravajyoti Patra** to National Institute of Technology Rourkela, during the academic session 2013-2015 is a record of bonafide research work carried out by him under my supervision and is worthy of consideration for the award of the degree of Masters of Technology in Mechanical Engineering with specialization in **Machine Design and Analysis.** The embodiment of this thesis has not been submitted to any Other University and/or Institute for the award of any degree or diploma.

Date: 1st June, 2015

Prof. Suraj Kumar Behera
Dept. of Mechanical Engineering
National Institute of Technology
Rourkela-769008

DEPARTMENT OF MECHANICAL ENGINEERING
NATIONAL INSTITUTE OF TECHNOLOGY
ROURKELA 769008

ACKNOWLEDGEMENT

It gives me immense pleasure to express my deep sense of gratitude to my supervisor **Prof. Suraj Kumar Behera** for his invaluable guidance, motivation, constant inspiration and above all for his ever co-operating attitude that enabled me in bringing up this thesis in the present form.

I am thankful to **Prof. S. S. Mohapatra**, Head, Department of Mechanical Engineering for providing all kinds of possible help and advice during the course of this work.

I would like to thank Mr. Himalaya Dawani M.Tech scholar, Department of Mechanical Engineering for his valuable suggestion during the research work. I am greatly thankful to all the staff members of the department and all my well-wishers, classmates and friends for their inspiration and help.

I would like to thanks my parents for their unconditional support, love and affection. Their encouragement and never ending kindness made everything easier to achieve.

Abstract

Gas lubrication has found a place of particular importance where it is necessary to keep the environment free from contamination by conventional lubricants. Pivot less tilting pad gas bearing mainly used for high speed rotors where whirling is the main issue. Each pad of the journal bearing forms a subsystem with its own local parameters to sustain the load. Basically three pads are used and each pad acts separately on the journal for better load carrying capacity. So during frequent start and stop application pads are coming in contacts protecting the bearing house. This paper contains aeronamic analysis of pivot less tilting pad gas journal bearing. Reynolds' equation is solved by finite difference method and Newton-Raphson method. Static characteristics like pressure profile, load carrying capacity, frictional force, coefficient of friction are calculated, and method to find dynamic parameters of stiffness and damping of a pivotless tilting pad gas journal bearing is shown. The author believes that such detail analysis on tilting pad gas journal bearing at different condition will help researchers around the world.

Keywords--Pivot less tilting pad gas bearing, Reynolds' equation, Newton-Raphson method, Load carrying capacity, pressure profile, stiffness and damping characteristics.

CONTENTS

TITLE	PAGE NO.
Certificate	ii
Acknowledgements	iii
Abstract	iv
Contents	v
List of Figures	vi
Nomenclature	vii
1. INTRODUCTION	**1**
1.1. Thesis Overview	1
1.2. Objective of the present work	2
1.3. Basic Concepts	2
1.4. Working Principle	4
2. LITERATURE REVIEW	**6**
3. NUMERICAL ANALYSIS	**10**
3.1. Generalised Fluid Equation and Reynolds Equation for Simple Gas Journal Bearing	10
3.1.1. Governing Equation	11
3.2. Pivot less tilting pad gas journal Bearing	14
3.2.1. Working Principle	15
3.2.2. Pressure distribution at the front face	16
3.2.3. Load Carrying Capacity	17
3.2.4. Frictional Shear Force	18
3.2.5. Coefficient of Friction	19
3.2.6. Flow Rate	19
3.2.7. Pressure distribution at the back face	19
3.2.8. Stiffness and Damping coefficients	20
3.3. Flow chart	27

4. RESULTS AND DISCUSSION **29**

4.1. Pressure Profile 29

4.2. Back Pad Pressure 31

4.3. Load Carrying Capacity 32

4.3.1. Load carrying capacity Vs. Eccentricity ratio 32

4.3.2. Load carrying capacity Vs. Pad Angle 33

4.3.3. Load carrying capacity Vs. Film thickness 34

4.3.4. Load carrying capacity Vs. Bearing number 35

4.3.5. Frictional Force Vs. Eccentricity Ratio 36

4.3.6. Coefficient of friction Vs. Eccentricity Ratio 36

4.3.7. Film thickness Ratio Vs. Eccentricity Ratio 37

5. CONCLUSION AND FUTURE ASPECTS **38**

REFERENCES **40**

LIST OF FIGURES

Fig. No.	Title	PAGE No.
Fig-1.1	Solid model of pivot less tilting pad gas journal bearing	5
Fig-1.2	Solid model of pivotless tilting pad	5
Fig-3.1	Infinitesimal element in Equilibrium	11
Fig-3.2	Pad and Rotor geometry	15
Fig-3.3	Skeleton model of Pivotless Tilting pad	15
Fig-4.1	3-D Non-dimensional Pressure distribution at the front face	29
Fig-4.2	Non-dimensional Pressure distribution on the pad surface along circumferential direction	30
Fig-4.3	Non-dimensional Pressure distribution on the pad surface along axial	30
Fig-4.4	3-D Non-dimensional total pressure distribution at the front face	31
Fig 4.5	3-D Non-dimensional Pressure distribution at back face of pad	31
Fig-4.6	Non-dimensional Back pressure distribution on the pad surface along circumferential direction	32
Fig-4.7	Variation of Non-dimensional pad load with eccentricity ratio	33
Fig-4.8	Variation of Non-dimensional pad load with pad angle	34
Fig-4.9	Variation of Non-dimensional pad load with film thickness ratio	34
Fig-4.10	Variation of Non-dimensional pad load with bearing number	35
Fig-4.11	Variation of Non-dimensional friction force with eccentricity Ratio	36
Fig-4.12	Variation of coefficient of friction with eccentricity Ratio	36
Fig-4.13	Variation of Non-dimensional film thickness ratio with eccentricity Ratio	37

Nomenclature

$\bar{B}_{rr}, \bar{B}_{r\theta}, \bar{B}_{\theta r}, \bar{B}_{\theta\theta}$	Non-dimensional Damping parameter $\left(\frac{cB_{rr}\omega}{W}, \frac{cB_{r\theta}\omega}{W}, \frac{cB_{\theta r}\omega}{W}, \frac{cB_{\theta\theta}\omega}{W}\right)$
c	Radial clearance (mm)
D	Diameter of bearing (mm)
D_w	Wedge width (mm)
dx, dy, dz	Unit length along X, Y, Z direction
e	Eccentricity (mm)
F_x	Horizontal reaction force (N)
F_y	Vertical reaction force (N)
f	Shear force (N)
$\bar{f}$	Non-dimensional shear force (F/Pa.RL)
H_0	Pad housing clearance (μm)
h	Oil film thickness (μm)
h_0	Oil film thickness due to static load (μm)
$\bar{h}$	Non-dimensional oil film thickness (h/c)
Δh	Oil film thickness due to dynamic load (μm)
$\bar{K}_{rr}, \bar{K}_{r\theta}, \bar{K}_{\theta r}, \bar{K}_{\theta\theta}$	Non-dimensional Stiffness parameter $\left(\frac{cK_{rr}}{W}, \frac{cK_{r\theta}}{W}, \frac{cK_{\theta r}}{W}, \frac{cK_{\theta\theta}}{W}\right)$
L	Pad length (mm)
M	Total number of grids along θ direction
N	Total number of grids along z direction
n	Number of revolution (rev/sec)
P	Pressure (M Pa)
P_0	Static Pressure (M Pa)
ΔP	Dynamic Pressure (M Pa)
P_a	Atmospheric pressure (M Pa)
$\bar{P}$	Non-dimensional Pressure (P/ P_a)
Q	Flow rate (mm^3/sec)
R	Radius of the Bearing (mm)
R_0	Radius of pad housing edge (mm)

r	Radius of the pad (mm)
r_0	Radius of pad housing (mm)
S	Sommerfeld Number
t	Time (sec)
U_0, U_1	Relative velocity in slider and pad in θ-direction (mm/sec)
V_1	Squeeze velocity between slider and pad (mm/sec)
u, v, w	Velocity in X, Y, Z direction (mm/sec)
W_r	Radial load (N)
W_t	Tangential load (N)
W	Total load (N)
$\bar{W}$	Non-dimensional Load carrying Capacity (W/Pa.RL)
x_0, y_0	Static equilibrium position (mm)
Z	Axial Direction
ω	Angular velocity (rad/sec)
ω'	Excitation Frequency (rad/sec)
ρ	Density of the fluid (kg/mm^3)
τ_x	Shear stress in X-direction (M Pa)
τ	Shear stress (M Pa)
$\bar{\tau}$	Non-dimensional shear stress (τ /Pa.RL)
μ	Dynamic viscosity (N-sec/mm^2)
μ_x	Coefficient of friction (F/W)
Λ	Bearing number $\left(\frac{6\mu\omega}{Pa}\left(\frac{R}{c}\right)^2\right)$
α	Effective pad angle
α'	Total pad angle (rad)
ε	Eccentricity ratio (e/c) (rad)
ε_s	Pad eccentricity ratio with respect to housing
θ	Circumferential Direction
θ_3	Effective angular extent of pad back face (rad)
δ	Angular Extent (Slot Angle) (rad)

1. INTRODUCTION: CHAPTER 1

Advances in technology have placed new demands on the support systems for many types of machine components. New design methods are evolving which based on combinations of conventional designs or follow new approaches. When point arises for load carrying capacity or relative motion the first thing that comes to our mind is the “Bearing”. Starting from toy to a high-speed jet, pen to super computer everywhere bearing shows its importance. So now days more emphasis given to bearing, starting from manufacturing of different parts, its assembly, and materials used, types of lubrication and a lot more.

Today’s market demands a bearing that is highly efficient in load carrying capacity, less frictional loss, less hazardous to the environment, low maintenance, with long life application. So as per requirement different types of bearing are available in the market & research is going on to improvise the properties of bearing.

In today’s scenario tribological loss is one of the biggest loss in industry application. So every effort is to minimize the loss and enhance the performance characteristics. Previously, the bearings that we used were fixed types of bearing. The clearance that we needed to maintain is very small that is up to a range of 1-10 μm. To maintain such small clearance in high speed is a very difficult task for the designers. So, they introduced different additional mechanisms like tilting pad, foils, textured in the bearing surface.

1.1 Thesis Overview:

Use of pads in journal bearing helps in better stabilization and distribution of pressure throughout the pad length. By using 3 to 4 pads, we’ll get extra number of convergent-divergent films unlike in the case of simple journal bearing where we get only one convergent-divergent film. The theoretical analysis is carried out by solving the non-dimensional Reynolds equation for gas bearing. In the current research air is used as the lubricating fluid.

Finite difference method is used to solve various static parameters like pressure for both front and back face of the pad, load carrying capacity, frictional force, coefficient of friction and dynamic parameters stiffness and damping characteristics. Effects of various parameters like eccentricity ratio, angle ratio, bearing number and film thickness on load carrying capacity is shown.

1.2 Objective of Present Work:

Current work aimed to study the aerodynamic analysis of pivot less tilting pad gas journal bearing. Followings are the main objectives of present work.

1. Development of numerical solution to finding various tribological static parameters such as pressure profile for both front and back face of the pad, load carrying capacity, flow rate, coefficient of friction etc.
2. Method to calculate dynamic characteristics like direct and cross coupled stiffness and damping parameters for tilting pad gas journal bearing is also shown.
3. Graphs have been plotted using various parameters for better understanding of performance.

1.3 Basic Concepts:

By forcing the fluid in between the gap of journal and bearing, friction can be reduced to a great amount. The method by which pressure applied is by two means. One is by externally applied pump and the other one is by creating the wedging action. Where the former is called the “fluid static” and the later one is “fluid dynamic”.

Almost all fluid static bearings use the same working principle. They use the externally pressurized fluid supply to run, also called as the “**passive fluid bearing”**.

Fluid dynamic bearing also called as “**self-acting bearing.** The pressure is generated by the wedging action due to which viscous shearing occurs. These bearings are simpler and cheaper

than the fluid static bearing. However, it requires a high standard of accuracy to maintain clearance between the journal and bearing**.**

1. Why gas bearing?

Gas bearing has evolved as the most acceptable solution for supporting small, high-speed turboexpander and turbocharger rotors. The reasons behind the use of gas bearing over oil lubricated bearing are low density and chemical stability [6]. As we know that gases are more chemically stable than liquids over a wide temperature range. Moreover, low viscosity causes low friction resulting lower heat generation. Other advantages like idealized to the bearing surface and radiation, and maintaining low noise level environment make the gas bearing more prominent over liquid bearings.

However, because of the low viscosity, gas bearing exhibit lower load carrying capacity and damping than the oil lubricated bearing, and, as a result, are more prone to instabilities. Both self-acting and externally pressurized bearings also suffer from the problem of half speed whirl instability [7].

2. Tilting Pad

In case of simple journal bearing to generate the pressure liquid lubricant forced into the gap between the journal and bearing. However, it requires a high standard of accuracy to maintain clearance between the journal and bearing. So during running at very high speed there is a metal to metal contact takes place that causes a material loss from the bearing surface. To avoid such condition pads are being used to protect the material also it helps to create more flexible operation by adjusting the pads to maintain the stability [16]. Also, there are other benefits of tilting pad over simple journal bearing that mentioned below.

- Higher reliability: - As this bearing required lesser parts to support the rotary motion, so the lesser frictional loss will involve. Also, there is some coating provided at the contact parts of the bearing.
- Less maintenance: - no lubrication so, lesser maintenance is required.

- Soft failure: - when a failure occurs, it confines the shaft movement and allows damage only to the pads and shaft surfaces.
- This kind of bearing is very much useful for high-speed operations and possesses well at high and low-temperature capabilities.

Tilting pad bearing categorised in 2 ways of using positioning the pads; one is "pivoted tilting pad" and another one is "pivotless tilting pad" bearing. In case of pivoted tilting pad, pivots are in line or point contact with the pad, whereas point contact is more acceptable because of the pads free align to the axis of the shaft. These bearings are also capable to accommodate circumferential and axial misalignment. Introducing a resilient support under one pad of a three pad bearing permits accommodation of centrifugal growth of the shaft and thermal changes in dimensions of both shaft and bearing housing.

The main bottleneck for the tilting pad bearing is the positioning of the pivot that is the real challenge for the engineers to find the actual position of the pivot. To avoid this problem pivot less tilting pad comes into play where wedges in the pads and another design mechanism overcome the requirement of the pivot.

1.4 Working Principle:

Pads of the tilting pad bearing have a very interesting structure. It consists of back face, front face, trailing edge, and a network of bleed and connecting holes that are capable of maintain the pressure and to carry the load. A solid model of pivot less tilting pad gas journal bearing given.

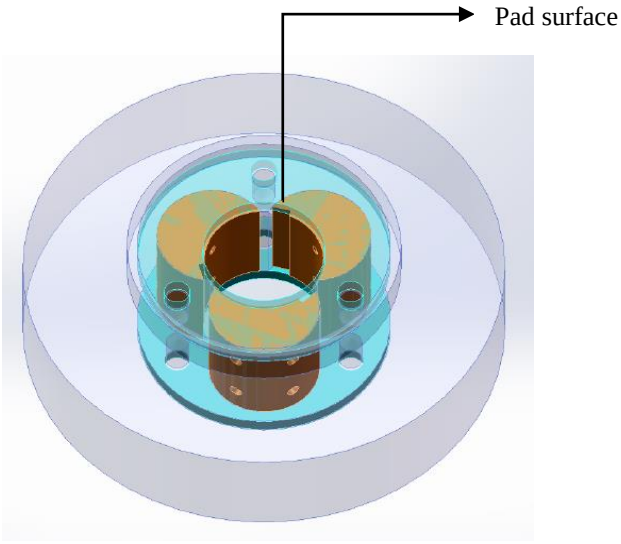

(Fig-1.1 Solid model of pivotless tilting pad gas journal bearing)

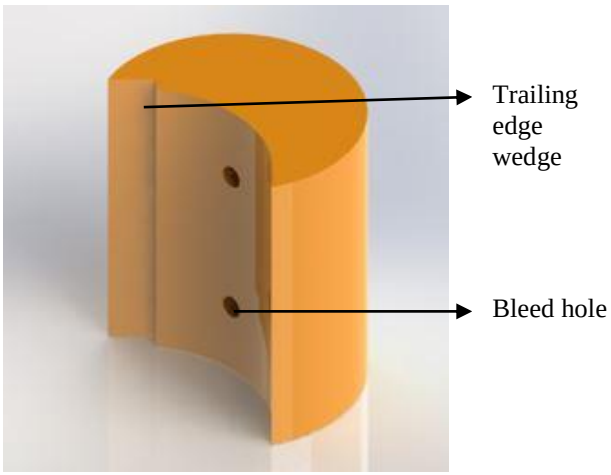

(Fig-1.2 Solid model of pivotless tilting pad)

Gas supplied to the bearing by means of external support. To maintain the pad position, some amount of gas passes through the holes that are made symmetrically across the pad length. It creates a pressure profile and the force caused due to the pressure passes through the geometric center of the circle defining the face. This geometry is acted as the imaginary pivot that divide the bearing area in two unequal parts. The main reason for this uneven distribution of the bearing area is for the presence of the trailing edge wedge. This difference in the area helps to adjust the pad to vanish the external forces and moments act upon it. There are 3 forces coming into picture aerodynamic load on the pad, frictional force in the pad and pressure force at the back face of the pad. The back pressure mainly depends on the clearance space present between the pad and bearing and it can be achieved by adjusting the bleed holes and geometry of the pad throughout the pad length.

2. Literature Review CHAPTER 2

Advances in technology have placed new demands on the support systems for many types of machine components, which demands compatible and environment-friendly bearing system. In recent days, one type of bearing that widely accepted is the use of tilting pad gas bearing. Gas lubrication has found a place of particular importance where it is necessary to keep the environment free from contamination by conventional lubricants. Use of pads in journal bearing helps in increasing the lifespan of machinery and also in better stabilization and distribution of pressure throughout the pad length.

The theoretical analysis of tilting pad bearing started over the last 50 years demonstrated by Lund using the highly nonlinear Reynolds' equation [8]. He used the finite difference solution of the Reynolds' equation to solve the parameters like pressure, load carrying capacity, stiffness and damping. In 1886, Reynolds gave his theory that explained the experimental results of Tower and Petroff assuming the flow to be isoviscous and laminar [5]. He also assumed that the pressure in the radial direction is very small as compared to the axial and circumferential direction can be neglected as the fluid film thickness is very small in the radial direction. By simplifying the Navier-Stokes and continuity equation, we can get the classic Reynolds equation [3].

$$\frac{d}{d\theta}\left(h^3\frac{dP}{d\theta}\right)+\frac{d}{dz}\left(h^3\frac{dP}{dz}\right)=6\mu\left[(U_0+U_1)+\frac{dh}{d\theta}+2V_1\right] \quad \text{..... (2.1)}$$

Where

P=developed pressure

θ, z =circumferential and axial direction

h =film thickness

U_0, U_1 = relative velocity of slider and pad in θ-direction

V_1 = squeeze velocity between slider and pad

μ =dynamic viscosity of fluid

Sommerfeld gave the first closed-form solution to the Reynolds equation. He also proposed a non-dimensional term by using various bearing parameters known as “Sommerfeld number(S)” or “Bearing Characteristics number” by assuming the lubricating flow to be laminar [7].

$$S = \left(\frac{r}{c}\right)^2 \frac{\mu N}{P}$$

Sulzer Brothers, the first Swiss company, to bring the aerodynamic journal and thrust bearings to the market used the oil lubricated bearings to support the cryogenic turbo expanders [3]. Later Hanny and Trepp used the tilting pad gas bearing in replace of radial oil bearing. Those bearings are consists of three pads. Each pad is capable of making a tilt over its pivot and producing a converging medium. Where the pressure generated in front and back face of the pads because of the converging medium are sufficient to carry the load.

In 1946, Hagg originally recognized the advantage of tilting pad bearing that removes the bearings that are the source of self-excited vibration. He experimented stabilizing features of tilting pad bearing with various pads by considering the flow to linear. This assumption did not valid for Reynolds equation.

Stodola and Hummel are first to quantify the dynamic response of oil lubricated bearing. Base on Sommerfeld closed form solution they were able to obtain the cross-coupled stiffness. However, they predict that an unstable rotor will vibrate with no bound.

Kingsbury and Michell independently invented Tilting pad bearing in 1916. In 1918, it used in H.M.S. Mackay of British Royal Navy. However, there are various demerits associated with the tilting pad bearing. Losses like higher parasitic losses, low load carrying capacity, lower operating speed and to overcome the demerits, designers used the noncircular bearing bores to enhance the stability margin.

Later Sternlicht gave the finite difference solution to solve the Reynolds equation to find the pressure. The force caused because of the pressure is perturbed to calculate the stiffness and damping parameters for fixed geometry journal bearing. Pinkus and Sternlicht gave the stability of rotors arranged with simple journal bearings in polar coordinates [3].

Tondl was experimenting on the instability of fixed geometric bearing and with the improvement in stability in case of fixed geometry bearing. His experiments directed to find out the direct stiffness, direct damping and cross-coupled stiffness terms. He also got some better results for the load carrying capacity and parasitic losses.

Even after the change in design criteria, there are some limitations where damping is dominated by the destabilizing forces. This situation appears when the operating frequency crosses the limit of twice to that of natural frequency. However, there were some improvements showed regarding the stabilizing effect, load carrying capacity and parasitic losses of the tilting pad bearing.

In 1964, Lund gave a landmark paper that reduced the dynamic coefficients synchronously [8]. He calculated the stiffness and damping for partial arc bearing and can be summed of vectorially to calculate the full bearing coefficient. The entire calculation was based on the fixed pad dynamic coefficients. Though this method was not the full proof solution to all pads, but it suited the computational condition of that time. This work was further extended to the thermodynamic and TEHD solutions for the tilting pad bearing.

Following the same basic method of Lund's approach, Orcutt found the turbulence effects in the lubricating film for the partial arc bearing. He calculated the turbulence effect by varying the number of pads and preload condition. He got an isotropic result for symmetric pad and load between pad conditions.

Nicholas and Kirk experimented on different stiffness and damping of four and five pads bearing by taking both 'load between pads' and 'load on pad' conditions and different pivot

positions [3]. They analyzed the unbalance and stability from the reduced stiffness and damping coefficient. He also explored the manufacturing tolerance to study the behavior of tilting pad under various conditions.

Jones and Martin directed their analysis towards minimum oil film thickness, average pad temperatures, bearing parasitic losses and synchronously reduced stiffness and damping coefficients for 3, 5, 7 tilting pad bearings.

Later Hashimoto gave the result regarding TEHD analysis on a large scale with two pad tilting pad bearing for a load between pads condition. A preload condition of 0.1, 0.2 were considered where pads were centrally pivoted.

Brockwell developed THD solution that included the pad thermal expansion and elastic deformation. Nicholas and Wygant took various design criteria to improve the dynamic characteristics for tilting pad bearing. He experimented with different pad materials for pivots and pads to improve the stiffness and damping coefficients.

3. NUMERICAL ANALYSIS CHAPTER 3

3.1 Generalised Fluid Equation & Reynolds Equation for Simple Gas Journal Bearing:

The generalised equation for simple journal bearing is the simplification of the general fluid mechanic equations governing the conservation of mass (continuity equation), momentum (Navier-Stokes equations), and energy (energy equation). The theory of aerodynamic bearing on a differential equation was derived by ***Osborne Reynold*.** Reynolds' theory explains the mechanism of lubrication through the generation of a viscous liquid film between the moving surfaces. There are two conditions for the occurrence of aerodynamic lubrication.

1. Two surfaces must move relative to each other with a sufficient velocity so that the lubricating film can carry the load.
2. Surfaces must be inclined at some angle to each other, i.e. if the surfaces are parallel the pressure will not sufficient to carry the load.

Reynolds equation is based on the following assumptions:

1. The lubricant obeys Newton's law of viscosity.
2. The inertia forces of air film are negligible.
3. The viscosity of the lubricant is constant.
4. The effect of curvature of the film with respect to film thickness is neglected. It can assumed that the film is so thin that the pressure is constant across the film thickness.
5. There is a continuous supply of lubricant.
6. There is no slip at the boundary.
7. The shaft and bearing are rigid.

3.1.1 Governing Equation:

An infinitesimally small element is having dimensions dx, dy and dz considered in the analysis. u and v are the velocities in x and y direction. 'τ_x'is the shear stress along the x direction and p is the fluid film pressure.

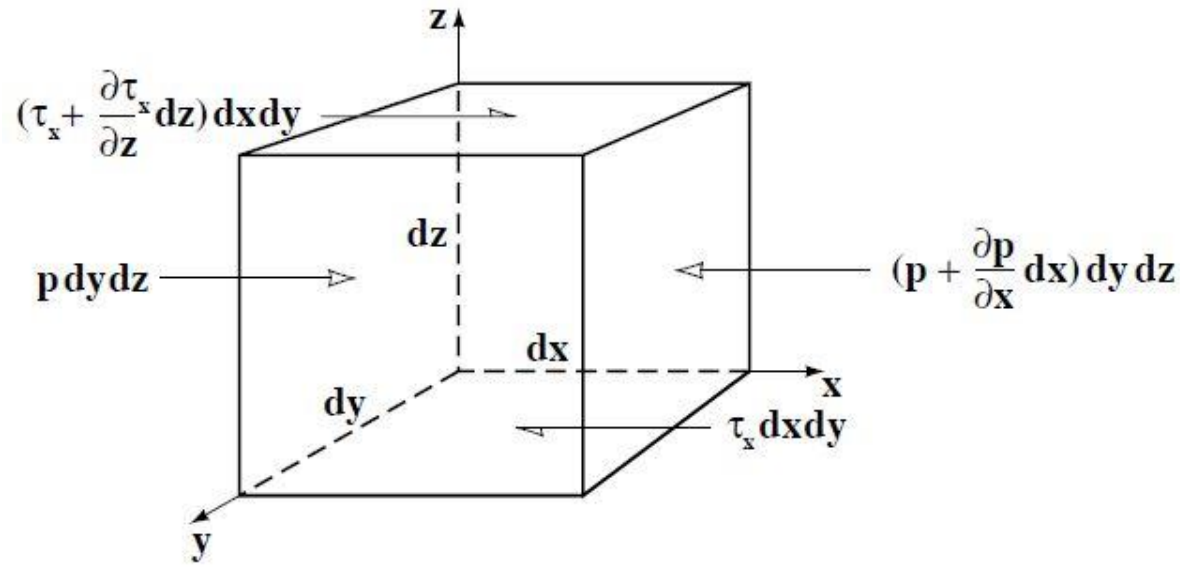

(Fig-3.1 Infinitesimal element in Equilibrium [18])

On balancing the forces in the x-direction, we get

$$P dy dz - \left(P + \frac{\partial P}{\partial x} dx \right) dy dz - \tau dx dz + \left(\tau_x + \frac{\partial \tau_x}{\partial y} dy \right) dx dz = 0 \qquad \text{..... (3.1)}$$

$$\Rightarrow \frac{\partial P}{\partial x} = \frac{\partial \tau_x}{\partial z} \qquad (\because \text{Assuming } dx dy dz \neq 0) \qquad \text{.... (3.2)}$$

From Newton's law of viscosity, we know that

$$\tau_x = \mu \frac{du}{dz} \qquad \text{..... (3.3)}$$

Substituting (2.3) into (2.2) we get

$$\frac{\partial P}{\partial x} = \mu \frac{\partial^2 u}{\partial z^2} \qquad \text{..... (3.4)}$$

Similarly balancing the forces in the y- direction, final result will be

$$\frac{\partial P}{\partial y} = \mu \frac{\partial^2 v}{\partial z^2} \qquad \text{.....} (3.5)$$

In z- direction

$$\frac{\partial P}{\partial z} = 0 \qquad \text{.....} (3.6)$$

As mention in the above assumption that, there is no slip or velocity at the boundary of the wedge, the boundary conditions are:

$u = U_2$ at $z = 0$

$u = U_1$ at $z = h$

Integrating twice the equation (3.4) and (3.5) we will find he value of velocities 'u and v' in the direction x and y as:

$$u = \left(\frac{z^2 - zh}{2\mu} \right) \frac{\partial P}{\partial x} + \left(U_1 - U_2 \right) \frac{z}{h} + U_2 \qquad \text{.....} (3.7)$$

$$v = \left(\frac{z^2 - zh}{2\mu} \right) \frac{\partial P}{\partial y} \qquad \text{.....} (3.8)$$

Equation of continuity can express as:

$$\frac{\partial \rho}{\partial t} + \frac{\partial}{\partial x}\left(\rho u\right) + \frac{\partial}{\partial y}\left(\rho v\right) + \frac{\partial}{\partial z}\left(\rho w\right) = 0 \qquad \text{.....} (3.9)$$

Integrating the above equation from 0 to h

$$\int_0^h \frac{\partial \rho}{\partial t} dz + \int_0^h \frac{\partial}{\partial x}\left(\rho u\right) dz + \int_0^h \frac{\partial}{\partial y}\left(\rho v\right) dz + \int_0^h \frac{\partial}{\partial z}\left(\rho w\right) dz = 0 \qquad \text{.....} (3.10)$$

Applying Leibnitz integration rule i.e.

$$\int_\alpha^\beta \frac{\partial u}{\partial x} dz = \frac{\partial}{\partial x} \int_\alpha^\beta u dz - u\left(\beta, x\right) \frac{d\beta}{dx} + u\left(\alpha, x\right) \frac{d\alpha}{dx}$$

Putting the value of 'u' and 'v' from equation (3.7) and (3.8) and applying in equation (3.10) a general expression for Reynolds' equation can be produced.

$$\frac{\partial}{\partial x}\left(\frac{\rho h^3}{12\mu}\frac{\partial P}{\partial x}\right)+\frac{\partial}{\partial y}\left(\frac{\rho h^3}{12\mu}\frac{\partial P}{\partial y}\right)=\frac{1}{2}\frac{\partial}{\partial x}\left[\rho\left(U_1+U_2\right)h\right]-\rho U_1\frac{\partial h}{\partial x}+\rho\left(w_2-w_1\right)+h\frac{\partial \rho}{\partial t} \quad \text{.....} \quad (3.11)$$

Where

$\frac{\partial}{\partial x}\left(\frac{\rho h^3}{12\mu}\frac{\partial P}{\partial x}\right)+\frac{\partial}{\partial y}\left(\frac{\rho h^3}{12\mu}\frac{\partial P}{\partial y}\right)$ = Net flow rate due to pressure gradient (Poiseulle term)

$\frac{1}{2}\frac{\partial}{\partial x}\left[\rho\left(U_1+U_2\right)h\right]$ =Net flow rate due to shear (Couette term)

$$=\frac{1}{2}\rho h\underbrace{\frac{\partial}{\partial x}\left(U_1+U_2\right)}_{\text{physical strech}}+\frac{1}{2}\rho\left(U_1+U_2\right)\underbrace{\frac{\partial h}{\partial x}}_{\substack{\text{physical}\\ \text{wedge}}}+\frac{1}{2}\left(U_1+U_2\right)h\underbrace{\frac{\partial \rho}{\partial x}}_{\substack{\text{density}\\ \text{wedge}}}$$

$\rho U_1\frac{\partial h}{\partial x}$ = Geometric squeeze term

$\rho\left(w_2-w_1\right)$ = Normal squeeze term

$h\frac{\partial \rho}{\partial t}$ =Local expansion

Equation (3.11) is the Cartesian form of the Reynolds equation. Taking suitable assumptions by neglecting the normal squeeze, local expansion, physical and density wedge terms, Reynolds' equation becomes

$$\frac{\partial}{\partial x}\left(\frac{\rho h^3}{12\mu}\frac{\partial P}{\partial x}\right)+\frac{\partial}{\partial y}\left(\frac{\rho h^3}{12\mu}\frac{\partial P}{\partial y}\right)=\frac{1}{2}U\frac{\partial(\rho h)}{\partial x} \quad \text{.....} \quad (3.12)$$

Where $U=U_2-U_1$

From the gas law, we know that

$$PV=mR_0T$$

$$\frac{m}{V}=\rho=\frac{P}{R_0T}$$

So, $\rho=f(P)$ where R_0 and T are constant values.

Reynolds equation in Cartesian form can rewrite as

$$\frac{\partial}{\partial x}\left(\frac{Ph^3}{12\mu}\frac{\partial P}{\partial x}\right)+\frac{\partial}{\partial y}\left(\frac{Ph^3}{12\mu}\frac{\partial P}{\partial y}\right)=\frac{1}{2}U\frac{\partial(Ph)}{\partial x} \quad \text{..... (3.13)}$$

By putting the values $x = R\theta, y = z$ the Cartesian form of Reynolds equation can be changed to Polar coordinates can be written as:

$$\frac{1}{R}\frac{\partial}{\partial\theta}\left(\frac{Ph^3}{12\mu}\frac{1}{R}\frac{\partial P}{\partial\theta}\right)+\frac{\partial}{\partial z}\left(\frac{Ph^3}{12\mu}\frac{\partial P}{\partial z}\right)=\frac{1}{2}\omega\frac{\partial(Ph)}{\partial\theta} \quad \text{..... (3.14)}$$

The boundary condition for the Reynolds equation given below [18].

$$P(0,z)=0$$

$$P\left(\theta,\pm\frac{L}{2}\right)=0 \qquad \text{(Gauge pressure)}$$

The above Reynolds equation is valid for laminar fluid flow and ideal no-slip boundary condition. The non-dimensional form of Reynolds equation in polar coordinates can written as:

$$\frac{\partial}{\partial\theta}\left(\bar{P}\bar{h}^3\frac{\partial\bar{P}}{\partial\theta}\right)+\left(\frac{R}{L}\right)^2\frac{\partial}{\partial Z}\left(\bar{P}\bar{h}^3\frac{\partial\bar{P}}{\partial Z}\right)=\Lambda\frac{\partial}{\partial\theta}(\bar{P}\bar{h}) \quad \text{..... (3.15)}$$

Where $\bar{h}=\frac{h}{c}=1+\varepsilon cos\theta$, $Z=\frac{z}{L}$

$$\Lambda=\frac{6\mu\omega}{P_a}\left(\frac{R}{c}\right)^2 \quad , \quad \bar{P}=\frac{P}{P_a}$$

‘ Λ ’ is known as ‘Bearing Number’.

3.2 Pivot less tilting pad gas journal Bearing:

The tilting pad journal bearing has evolved as one of the most effective means of stabilizing high-speed rotors against half speed whirl. Because of its inherent quality of self-alignment and stability characteristics, it has a wide range of application starting from cryogenic turbo expander to high-temperature gas circulators for nuclear reactors [7].

3.2.1 Working principle:

This chapter deals with the aerodynamic analysis of a pivotless tilting pad gas journal bearing. The more common difficulty in pivoted tilting pad is the positioning of the pivot. Pivots are of two forms; one is point support, and other is line contact between the pivot and pad among which former is most accepted [6].

Each pad in a pivotless tilting pad bearing consists of three things, front face with a wedge that forms the bearing surface, back face and a network of holes. A wedge is present in the front face along with the network of holes that helps to eliminate the limitation of positioning the pivot. When gas supplied to the bearing by external means, a small amount of gas passes to the back face of the pad. This back pad pressure adjust the pad and to generate the pressure at the back face. The force caused due to the pressure passes through the geometric center of the circle defining the face. This geometry acted as the imaginary pivot that divides the bearing surface into two unequal parts until all the forces and moments vanish.

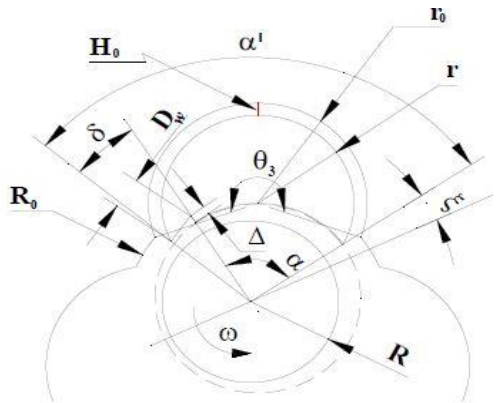

(Fig-3.2 Pad and Rotor geometry [4])

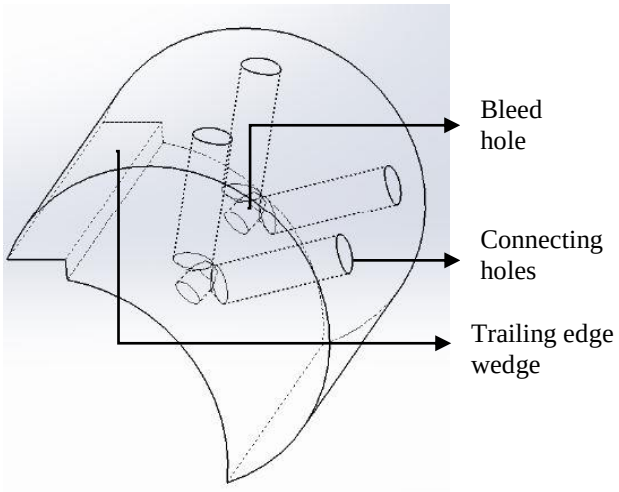

(Fig-3.3 Skeleton model of a Pivotless Tilting Pad)

The governing equation:

For better understanding, the entire analysis is broken into two parts. Here the pressure profile for front and back face of the pad is calculated separately. The effective bearing surface along with the rotor is treated as a partial arc bearing and pressure at the back face of the bearing is solely because of the aerostatic means.

3.2.2 Pressure distribution at the front face:

In tilting pad bearing pressure is calculated by considering the pad to be a partial arc journal bearing. The pressure that is calculated is only for a single pad and to calculate the total pressure we need to sum up the effect of individual pad. The dimensionless Reynolds equation for partial arc gas journal bearing is same as that of equation (3.15).

$$\frac{\partial}{\partial\theta}\left[\bar{P}\bar{h}^3\frac{\partial\bar{P}}{\partial\theta}\right]+\left(\frac{R}{L}\right)^2\frac{\partial}{\partial Z}\left[\bar{P}\bar{h}^3\frac{\partial\bar{P}}{\partial Z}\right]=\Lambda\frac{\partial}{\partial\theta}\left(\bar{P}\bar{h}\right)$$

By using partial differentiation to equation (3.15), we get,

$$\left(\frac{\partial\bar{P}}{\partial\theta}\right)^2+\frac{3\bar{P}}{\bar{h}}\frac{\partial\bar{P}}{\partial\theta}\frac{\partial\bar{h}}{\partial\theta}+\bar{P}\frac{\partial^2\bar{P}}{\partial^2\theta}+\left(\frac{R}{L}\right)^2\left[\left(\frac{\partial\bar{P}}{\partial Z}\right)^2+\bar{P}\frac{\partial^2\bar{P}}{\partial Z^2}\right]=\frac{\Lambda}{\bar{h}^2}\frac{\partial\bar{P}}{\partial\theta}+\frac{\Lambda\bar{P}}{\bar{h}^3}\frac{\partial\bar{h}}{\partial\theta} \quad \text{.....} (3.16)$$

The non-dimensional pressure can calculated by using the 'Finite Difference Method' in MATLAB. The principle of the Finite Difference Method to find the partial derivative of a differential equation is approximated by linear combinations of functional values at the grid points. In this paper, we use the 'central difference operator' for finite difference method.

Finite Difference Operators:

$$\left.\begin{aligned}
\frac{\partial\bar{P}}{\partial\theta}&=\frac{\bar{P}_{i+1,j}-\bar{P}_{i-1,j}}{2\Delta\theta}\\
\frac{\partial^2\bar{P}}{\partial\theta^2}&=\frac{\bar{P}_{i+1,j}+\bar{P}_{i-1,j}-2\bar{P}_{i,j}}{\Delta\theta^2}\\
\frac{\partial\bar{P}}{\partial Z}&=\frac{\bar{P}_{i,j+1}-\bar{P}_{i,j-1}}{2\Delta Z}\\
\frac{\partial^2\bar{P}}{\partial Z^2}&=\frac{\bar{P}_{i,j+1}+\bar{P}_{i,j-1}-2\bar{P}_{i,j}}{\Delta Z^2}
\end{aligned}\right\} \quad \text{.....} (3.17)$$

Using finite difference operators in equation (3.16), from equation (3.17), we will get a quadratic equation in terms of pressure and solving that equation we get pressure at each grid point.

$$\bar{P}_{i,j}{}^{2} - 2E_{i,j}\bar{P}_{i,j} + F_{i,j} = 0 \qquad \text{.....} \quad (3.18)$$

Where

$$E_{i,j} = \frac{\bar{P}_{i+1,j} + \bar{P}_{i-1,j}}{2D(\Delta\theta)^2} + \frac{3\left(\bar{P}_{i+1,j} - \bar{P}_{i-1,j}\right)}{4D\bar{h}_i(\Delta\theta)}\left(\frac{d\bar{h}}{d\theta}\right)_i + \left(\frac{R}{L}\right)^2 \frac{\bar{P}_{i,j+1} + \bar{P}_{i,j-1}}{2D(\Delta Z)^2} - \frac{\Lambda}{2D\bar{h}_i^3}\left(\frac{d\bar{h}}{d\theta}\right)_i$$

$$F_{i,j} = \frac{\Lambda(\bar{P}_{i+1,j} - \bar{P}_{i-1,j})}{2D\bar{h}_i^2(\Delta\theta)} - \frac{\left(\bar{P}_{i+1,j} - \bar{P}_{i-1,j}\right)^2}{4D(\Delta\theta)^2} - \left(\frac{R}{L}\right)^2 \frac{(\bar{P}_{i,j+1} - \bar{P}_{i,j-1})^2}{4D(\Delta Z)^2}$$

$$D = 2\left[\frac{1}{(\Delta\theta)^2} + \left(\frac{R}{L}\right)^2 \frac{1}{(\Delta Z)^2}\right]$$

$$\Delta\theta = \frac{\alpha}{M} \quad , \Delta z = \frac{1}{N}$$

The boundary conditions required to solve equation (3.18) are given below.

$$\bar{P}(\xi, Z) = \bar{P}(\xi + \alpha, Z) = 1$$
$$\bar{P}(\theta, \pm 0.5) = 1$$

The boundary conditions indicate that the pressure at the edge of the pad is ambient.

The only difference in simple journal bearing and tilting pad bearing is in the value of '$\Delta\theta$'. The value of $\Delta\theta$ depends on the value of effective pad angle in case of a tilting pad bearing which is denoted by (α) and for simple journal bearing, it depends on the entire bearing angle. By solving the equation (3.18) for pressure using Newton –Raphson method, in Matlab, pressure profile for the front face of the pad, can be found out.

3.2.3 Load Carrying Capacity:

The force due to bearing pressure can be resolved into two components along and normal to the maximum film thickness direction on the elemental area. That can be integrated over the entire pad surface to calculate the load carrying capacity of a single pad in the respective

direction. W_r and W_t are the load capacities along and normal to the maximum film thickness direction respectively. The non-dimensional form of the load carrying capacity can be expressed as:

$$\overline{W_r} = \frac{W_r}{P_a RL} = \int_{-0.5}^{0.5} \int_{\xi}^{\xi+\alpha} \bar{P} \cos\theta \, d\theta \, dZ$$
$$\overline{W_t} = \frac{W_t}{P_a RL} = \int_{-0.5}^{0.5} \int_{\xi}^{\xi+\alpha} \bar{P} \sin\theta \, d\theta \, dZ \quad \text{..... (3.19)}$$

The magnitude of total non-dimensional aerodynamic load capacity can be expressed as:

$$\bar{W} = \frac{W}{P_a RL} = \sqrt{\bar{W}_r^2 + \bar{W}_t^2} \quad \text{..... (3.20)}$$

3.2.4 Frictional shear force:

Shearing action caused by air on the surface of the pad creates the frictional shear stress.

The stress due to viscous friction can be written as

$$\tau = \mu \frac{u}{h} + \frac{h}{2R} \frac{\partial P}{\partial \theta}$$

Non-dimensional form can be written as:

$$\bar{\tau} = \frac{\tau}{P_a RL} = \frac{1}{\bar{h}} + \frac{3}{\Lambda} \frac{\partial \bar{P}}{\partial \theta} \quad \text{..... (3.21)}$$

By integrating the frictional shear stress throughout the pad length we can found the value of frictional shear force.

$$f = \int_{-0.5}^{0.5} \int_{\xi}^{\xi+\alpha} \tau R \, d\theta \, dz$$

The non-dimensional form can written as

$$\bar{f} = \int_{-0.5}^{0.5} \int_{\xi}^{\xi+\alpha} \bar{\tau} \, d\theta \, dZ \quad \text{..... (3.22)}$$

3.2.5 Coefficient of Friction:

Ratio between frictional shear force and load carrying capacity is called as coefficient of frictional force. Where coefficient of frictional force,

$$\bar{\mu} = \frac{\bar{f}}{\bar{W}} \qquad \text{..... (3.23)}$$

3.2.6 Flow rate:

Proper flow of lubricating oil into the journal bearing system not only helps to carry out the heat but also helps to stabilise and to control the pressure of the entire bearing system. It also protects the bearing from accumulating the dust particles inside the bearing. So, flow rate has a great influence on bearing life.

Flow rate can express as:

$$Q = 2\int_0^{\pi} \frac{h^3}{12\mu}\left(\frac{\partial P}{\partial z}\right)_{\pm\frac{L}{2}} R d\theta$$

$$\bar{Q} = \frac{P_a c^3}{6\mu}\left(\frac{R}{L}\right)\int_0^{\pi} \bar{h}^3 \frac{\partial \bar{P}}{\partial Z} d\theta \qquad \text{..... (3.24)}$$

3.2.7 Pressure distribution at the back face:

Pressure distribution at the back face of the pad is by aerostatic means. Back pad pressure can be generated by supplying gas through the network of connecting hoes and bleed holes. This network of holes plays an important role for elimination of pivot from the back surface of the pad. Because of the symmetry only one half of the bearing can be taken in to consideration. The non-dimensional Reynolds equation for back face of the pad can be expressed as

$$\frac{\partial}{\partial\theta}\left[\bar{P}\bar{H}^3\frac{\partial\bar{P}}{\partial\theta}\right] + \left(\frac{r}{L}\right)^2 \frac{\partial}{\partial Z}\left[\bar{P}\bar{H}^3\frac{\partial\bar{P}}{\partial Z}\right] = 0 \qquad \text{..... (3.25)}$$

Using FDM

$$P_{i,j}{}^2 - 2E_{i,j}P_{i,j} - F_{i,j} = 0 \qquad \text{..... (3.26)}$$

Where

$$E_{i,j} = \frac{\bar{P}_{i+1,j} + \bar{P}_{i-1,j}}{2D(\Delta\theta)^2} + \frac{3\left(\bar{P}_{i+1,j} - \bar{P}_{i-1,j}\right)}{4D\bar{H}_i(\Delta\theta)}\left(\frac{d\bar{H}}{d\theta}\right)_i + \left(\frac{r}{L}\right)^2 \frac{\bar{P}_{i,j+1} + \bar{P}_{i,j-1}}{2D(\Delta Z)^2}$$

$$F_{i,j} = \frac{\left(\bar{P}_{i+1,j} - \bar{P}_{i-1,j}\right)^2}{4D(\Delta\theta)^2} + \left(\frac{r}{L}\right)^2 \frac{(\bar{P}_{i,j+1} - \bar{P}_{i,j-1})^2}{4D(\Delta Z)^2}$$

$$\bar{H} = 1 - \varepsilon_s \cos\left(\frac{\theta_3}{2} - \theta\right)$$

$$\Delta\theta = \frac{\theta_3}{2M} \quad , \Delta z = \frac{1}{2N}$$

$\bar{H}$ is the dimensionless film thickness between the pad back face and bearing house.

3.2.8 Stiffness and damping coefficients:

The resistance to deforming against the applied load is called as stiffness. Similarly damping is a parameter that restricts the present motion by absorbing the energy. In a journal bearing system, damping can be produced by dissipating the energy that stored in the rotary motion. In the modern era the need to increasing speed yet the reliable operation increases day by day and to achieve this we have to predict the dynamic response and stability of a rotor-bearing system accurately. In fluid-film bearing fluid-film is a thin film that separates the bearing to keep in contact with the journal, it acts like a spring and provides damping. Stiffness and damping properties of the fluid-film bearing alter the critical speed and out of balance response of the rotor. The stability of a rotor is mostly affected by the dynamic characteristics of the bearing. So the dynamic coefficients produced by small amplitude whirl, can be calculated by using the finite difference method, considering the dynamic pressure.

Considering X-axis and Y-axis to be vertical and horizontal direction respectively, the force 'F' is a function of x, y, $\dot{x}, \dot{y}$. Where x, y and $\dot{x}, \dot{y}$ are the instantaneous displacements and velocities along X and Y direction respectively [8]. F can be resolved into F_x, F_y along the negative X-axis and Y-axis respectively.

A first order Taylor series expansion is required to define the vertical and horizontal forces as linear functions of instantaneous bearing center displacements (x, y) and velocities ($x^{'}, y^{'}$)

$$F_x = F_{x_0} + \left(\frac{\partial F_x}{\partial x}\right)_0 \Delta x + \left(\frac{\partial F_x}{\partial y}\right)_0 \Delta y + \left(\frac{\partial F_x}{\partial x'}\right)_0 \Delta x' + \left(\frac{\partial F_x}{\partial y'}\right)_0 \Delta y' \quad \text{..... (3.27)}$$

$$F_y = F_{y_0} + \left(\frac{\partial F_y}{\partial x}\right)_0 \Delta x + \left(\frac{\partial F_y}{\partial y}\right)_0 \Delta y + \left(\frac{\partial F_y}{\partial x'}\right)_0 \Delta x' + \left(\frac{\partial F_y}{\partial y'}\right)_0 \Delta y' \quad \text{..... (3.28)}$$

At static equilibrium condition there is only a static load W is acting, so the force system can be expressed as

$$F_{x_0} = F_x\left(x_0, y_0, 0, 0\right) = W$$
$$F_{y_0} = F_y\left(x_0, y_0, 0, 0\right) = 0$$

For small amplitudes Δx and Δy the dynamic force equation can be expressed as

$$\left.\begin{aligned} \Delta F_x &= K_{xx}\Delta x + K_{xy}\Delta y + B_{xx}\Delta x' + B_{xy}\Delta y' \\ \Delta F_y &= K_{yx}\Delta x + K_{yy}\Delta y + B_{yx}\Delta x' + B_{yy}\Delta y' \end{aligned}\right\} \quad \text{..... (3.29)}$$

A harmonic perturbation method is used to solve the dynamic coefficients. The perturbation is a mathematical method to find an approximate solution where getting an exact solution is difficult. Such problems are consisting of two parts. One is ‘solvable part’ and other is ‘perturbation part’. A small term added to the exactly solvable problem to get the approximate solution.

So the oil film thickness and pressure because of the small harmonic motion [20] can be expressed as

$$h = h_0 + \Delta h.e^{i\omega t} \quad \text{..... (3.30)}$$

$$P = P_0 + \Delta P.e^{i\omega t} \quad \text{..... (3.31)}$$

Applying equation (3.29) and (3.30) in equation (3.14) the zeroth order equation in polar form can written as:

Zeroth order:

$$\frac{1}{R}\frac{\partial}{\partial\theta}\left(P_0{h_0}^3\frac{1}{R}\frac{\partial P_0}{\partial\theta}\right)+\frac{\partial}{\partial z}\left(P_0{h_0}^3\frac{\partial P_0}{\partial z}\right)=6\mu\omega\frac{\partial(P_0h_0)}{\partial\theta}\,. \qquad \text{..... (3.32)}$$

For dynamic calculation the Reynolds equation can written as:

$$\frac{1}{R}\frac{\partial}{\partial\theta}\left(\frac{Ph^3}{12\mu}\frac{1}{R}\frac{\partial P}{\partial\theta}\right)+\frac{\partial}{\partial z}\left(\frac{Ph^3}{12\mu}\frac{\partial P}{\partial z}\right)=\frac{1}{2}\omega\frac{\partial}{\partial\theta}(Ph)+\frac{\partial}{\partial t}(Pt)$$

Applying equation (3.29) and (3.30) in above equation the First order equation in polar form can written as:

First order:

Along X-direction

$$\begin{aligned}&\frac{1}{R}\frac{\partial}{\partial\theta}\left(p_0{h_0}^3\frac{1}{R}\frac{\partial P_x}{\partial\theta}+P_x{h_0}^3\frac{1}{R}\frac{\partial p_0}{\partial\theta}\right)+\frac{\partial}{\partial z}\left(p_0{h_0}^3\frac{\partial P_x}{\partial z}+P_x{h_0}^3\frac{\partial p_0}{\partial z}\right)+6\mu U\frac{1}{R}\frac{\partial(P_xh_0)}{\partial\theta}+12\mu i\omega'(h_0P_x)\\&=-\frac{1}{R}\frac{\partial}{\partial\theta}\left(3P_0{h_0}^2\frac{\partial P_0}{\partial\theta}\cos\theta\right)-\frac{\partial}{\partial z}\left(3P_0{h_0}^2\frac{\partial P_0}{\partial z}\cos\theta\right)+6\mu U\frac{1}{R}\frac{\partial(P_0\cos\theta)}{\partial\theta}+12\mu i\omega'(P_0\cos\theta)\end{aligned} \qquad \text{..(3.33)}$$

Along Y-direction

$$\begin{aligned}&\frac{1}{R}\frac{\partial}{\partial\theta}\left(P_0{h_0}^3\frac{1}{R}\frac{\partial P_y}{\partial\theta}+p_y{h_0}^3\frac{1}{R}\frac{\partial P_0}{\partial\theta}\right)+\frac{\partial}{\partial z}\left(P_0{h_0}^3\frac{\partial P_y}{\partial z}+P_y{h_0}^3\frac{\partial P_0}{\partial z}\right)+6\mu U\frac{1}{R}\frac{\partial(P_yh_0)}{\partial\theta}+12\mu i\omega'(h_0P_y)\\&=-\frac{1}{R}\frac{\partial}{\partial\theta}\left(3P_0{h_0}^2\frac{1}{R}\frac{\partial P_0}{\partial\theta}\sin\theta\right)-\frac{\partial}{\partial z}\left(3P_0{h_0}^2\frac{\partial P_0}{\partial z}\sin\theta\right)+6\mu U\frac{1}{R}\frac{\partial(P_0\sin\theta)}{\partial\theta}+12\mu i\omega'(P_0\sin\theta)\end{aligned} \qquad \text{..(3.34)}$$

The boundary condition that required for zeroth and first order equations are,

(For zeroth order)

$$\left.\begin{aligned}P_0(y,0)&=P_0(y,L)\\P_0(\theta_1,z)&=P_0(\theta_2,z)\end{aligned}\right\}=P_a$$

$$\frac{\partial P_0(\theta_1,z)}{\partial y}=\frac{\partial P_0(\theta_2,z)}{\partial y}$$

(For first order)

$$\left.\begin{aligned}P_{x,y}(y,0)&=P_{x,y}(y,L)\\P_{x,y}(\theta_1,z)&=P_{x,y}(\theta_2,z)\end{aligned}\right\}=0$$

$$\frac{\partial P_{x,y}(\theta_1,z)}{\partial y}=\frac{\partial P_{x,y}(\theta_2,z)}{\partial y}$$

The non-dimensional form for the zeroth and first order equation can written as:

For zeroth order:

$$\left(\frac{\partial \bar{P}_0}{\partial \theta}\right)^2+\frac{3\bar{P}_0}{\bar{h}}\frac{\partial \bar{P}_0}{\partial \theta}\frac{\partial \bar{h}}{\partial \theta}+\bar{P}_0\frac{\partial^2 \bar{P}_0}{\partial^2 \theta}+\left(\frac{R}{L}\right)^2\left[\left(\frac{\partial \bar{P}_0}{\partial Z}\right)^2+\bar{P}_0\frac{\partial^2 \bar{P}_0}{\partial Z^2}\right]=\frac{\Lambda}{\bar{h}^2}\frac{\partial \bar{P}_0}{\partial \theta}+\frac{\Lambda \bar{P}_0}{\bar{h}^3}\frac{\partial \bar{h}}{\partial \theta}$$

..... (3.35)

For First order:

Along X-direction

$$\frac{\partial}{\partial \theta}\left[\bar{P}_0\bar{h}^3\frac{\partial \bar{P}_x}{\partial \theta}+\bar{P}_x\bar{h}^3\frac{\partial \bar{P}_0}{\partial \theta}\right]+\left(\frac{R}{L}\right)^2\frac{\partial}{\partial Z}\left[\bar{P}_0\bar{h}^3\frac{\partial \bar{P}_x}{\partial Z}+\bar{P}_x\bar{h}^3\frac{\partial \bar{P}_0}{\partial Z}\right]+\Lambda\frac{\partial}{\partial \theta}\left(\bar{P}_x\bar{h}\right)+i2\Lambda'\bar{P}_x\bar{h}$$
$$=-3\frac{R}{c}\left[\frac{\partial}{\partial \theta}\left(\bar{P}_0\bar{h}^2\frac{\partial \bar{P}_0}{\partial \theta}\cos\theta\right)+\left(\frac{R}{L}\right)^2\cos\theta\frac{\partial}{\partial Z}\left(\bar{P}_0\bar{h}^2\frac{\partial \bar{P}_0}{\partial Z}\right)\right]+\left(\frac{R}{c}\right)\left[\Lambda\frac{\partial}{\partial \theta}\left(\bar{P}_0\cos\theta\right)+i2\Lambda'\bar{P}_0\cos\theta\right]$$

..... (3.36)

Along Y-direction

$$\frac{\partial}{\partial \theta}\left[\bar{P}_0\bar{h}^3\frac{\partial \bar{P}_y}{\partial \theta}+\bar{P}_y\bar{h}^3\frac{\partial \bar{P}_0}{\partial \theta}\right]+\left(\frac{R}{L}\right)^2\frac{\partial}{\partial Z}\left[\bar{P}_0\bar{h}^3\frac{\partial \bar{P}_y}{\partial Z}+\bar{P}_y\bar{h}^3\frac{\partial \bar{P}_0}{\partial Z}\right]+\Lambda\frac{\partial}{\partial \theta}\left(\bar{P}_y\bar{h}\right)+i2\Lambda'\bar{P}_y\bar{h}$$
$$=-3\frac{R}{c}\left[\frac{\partial}{\partial \theta}\left(\bar{P}_0\bar{h}^2\frac{\partial \bar{P}_0}{\partial \theta}\sin\theta\right)+\left(\frac{R}{L}\right)^2\sin\theta\frac{\partial}{\partial Z}\left(\bar{P}_0\bar{h}^2\frac{\partial \bar{P}_0}{\partial Z}\right)\right]+\left(\frac{R}{c}\right)\left[\Lambda\frac{\partial}{\partial \theta}\left(\bar{P}_0\sin\theta\right)+i2\Lambda'\bar{P}_0\sin\theta\right]$$

..... (3.37)

Where

$$\bar{h}=\frac{h}{c}=1+\varepsilon\cos\theta,\quad Z=\frac{z}{L},\quad \bar{P}_x=\frac{P_xR}{P_a},\quad \bar{P}_0=\frac{P_0}{P_a}$$

$$\Lambda=\frac{6\mu\omega}{P_a}\left(\frac{R}{c}\right)^2,\quad \Lambda'=\frac{6\mu\omega'}{P_a}\left(\frac{R}{c}\right)^2,\quad \bar{P}=\frac{P}{P_a},\quad \bar{P}_y=\frac{P_yR}{P_a}$$

Using the finite difference method with the help of central difference operator the partial derivative terms can be expressed as

Finite Difference Operators:

$$\frac{\partial \overline{P_y}}{\partial \theta}=\frac{\overline{P_{y_{i+1,j}}}-\overline{P_{y_{i-1,j}}}}{2\Delta\theta};\qquad \frac{\partial \overline{P_x}}{\partial \theta}=\frac{\overline{P_{x_{i+1,j}}}-\overline{P_{x_{i-1,j}}}}{2\Delta\theta};\qquad \frac{\partial \overline{P_y}}{\partial \theta}=\frac{\overline{P_{y_{i+1,j}}}-\overline{P_{y_{i-1,j}}}}{2\Delta\theta};$$

$$\frac{\partial^2 \overline{P_y}}{\partial \theta^2}=\frac{\overline{P_{y_{i+1,j}}}+\overline{P_{y_{i-1,j}}}-2\overline{P_{y_{i,j}}}}{\Delta\theta^2};\quad \frac{\partial^2 \overline{P_x}}{\partial \theta^2}=\frac{\overline{P_{x_{i+1,j}}}+\overline{P_{x_{i-1,j}}}-2\overline{P_{x_{i,j}}}}{\Delta\theta^2};\quad \frac{\partial^2 \overline{P_y}}{\partial \theta^2}=\frac{\overline{P_{y_{i+1,j}}}+\overline{P_{y_{i-1,j}}}-2\overline{P_{y_{i,j}}}}{\Delta\theta^2};$$

$$\frac{\partial \overline{P_y}}{\partial Z}=\frac{\overline{P_{y_{i,j+1}}}-\overline{P_{y_{i,j-1}}}}{2\Delta Z};\qquad \frac{\partial \overline{P_x}}{\partial Z}=\frac{\overline{P_{x_{i,j+1}}}-\overline{P_{x_{i,j-1}}}}{2\Delta Z};\qquad \frac{\partial \overline{P_y}}{\partial Z}=\frac{\overline{P_{y_{i,j+1}}}-\overline{P_{y_{i,j-1}}}}{2\Delta Z};$$

$$\frac{\partial^2 \overline{P_y}}{\partial Z^2}=\frac{\overline{P_{y_{i,j+1}}}+\overline{P_{y_{i,j-1}}}-2\overline{P_{y_{i,j}}}}{\Delta Z^2};\quad \frac{\partial^2 \overline{P_x}}{\partial Z^2}=\frac{\overline{P_{x_{i,j+1}}}+\overline{P_{x_{i,j-1}}}-2\overline{P_{x_{i,j}}}}{\Delta Z^2};\quad \frac{\partial^2 \overline{P_y}}{\partial Z^2}=\frac{\overline{P_{y_{i,j+1}}}+\overline{P_{y_{i,j-1}}}-2\overline{P_{y_{i,j}}}}{\Delta Z^2};$$

Using the finite difference operators to the zeroth and first order equation can be expressed as:

Zeroth order

Calculation of P_0:

$$P_{0_{i,j}}{}^2-2A_{i,j}P_{0_{i,j}}+B_{i,j}=0 \qquad \text{.....} (3.38)$$

$$A_{i,j}=\frac{\bar{P}_{0_{i+1,j}}+\bar{P}_{0_{i-1,j}}}{2D(\Delta\theta)^2}+\frac{3\left(\bar{P}_{0_{i+1,j}}-\bar{P}_{0_{i-1,j}}\right)}{4D\bar{h}_i(\Delta\theta)}\left(\frac{d\bar{h}}{d\theta}\right)_i+\left(\frac{R}{L}\right)^2\frac{\bar{P}_{0_{i,j+1}}+\bar{P}_{0_{i,j-1}}}{2D(\Delta Z)^2}-\frac{\Lambda}{2D\bar{h}_i^3}\left(\frac{d\bar{h}}{d\theta}\right)_i$$

$$B_{i,j}=\frac{\Lambda(\bar{P}_{0_{i+1,j}}-\bar{P}_{0_{i-1,j}})}{2D\bar{h}_i^2(\Delta\theta)}-\frac{\left(\bar{P}_{0_{i+1,j}}-\bar{P}_{0_{i-1,j}}\right)^2}{4D(\Delta\theta)^2}-\left(\frac{R}{L}\right)^2\frac{(\bar{P}_{0_{i,j+1}}-\bar{P}_{0_{i,j-1}})^2}{4D(\Delta Z)^2}$$

$$D=2\left[\frac{1}{(\Delta\theta)^2}+\left(\frac{R}{L}\right)^2\frac{1}{(\Delta Z)^2}\right]$$

$$\Delta\theta=\frac{\alpha}{M}\quad,\Delta Z=\frac{1}{N}$$

First Order

Calculation of P_x:

Along X-direction

$$\bar{P}_{x_{i,j}}=\frac{B1+C1+D1+E1}{A1} \qquad \text{.....} (3.39)$$

Where A1= $\left[3\bar{h}^2 \frac{\partial \bar{h}}{\partial \theta} \frac{\partial \bar{P}_0}{\partial \theta} + \bar{h}^3 \frac{\partial^2 \bar{P}_0}{\partial \theta^2} + \left(\frac{R}{L}\right)^2 \bar{h}^3 \frac{\partial^2 \bar{P}_0}{\partial Z^2} - \bar{P}_0 \bar{h}^3 \left(\frac{2}{\Delta\theta^2} + \left(\frac{R}{L}\right)^2 \frac{2}{\Delta Z^2} \right) + \Lambda \frac{\partial \bar{h}}{\partial \theta} + i2\Lambda' \bar{h} \right]$

B1= $-\frac{\partial \bar{P}_x}{\partial \theta} \left[2 \frac{\partial \bar{P}_0}{\partial \theta} \bar{h}^3 + 3\bar{h}^2 \frac{\partial \bar{h}}{\partial \theta} \bar{P}_0 \right] - \bar{h}^3 \bar{P}_0 \frac{\bar{P}_{x_{i+1,j}} + \bar{P}_{x_{i-1,j}}}{\partial \theta^2} - \Lambda \bar{h} \frac{\partial \bar{P}_x}{\partial \theta}$

C1= $-\left(\frac{R}{L}\right)^2 \bar{h}^3 \left[2 \frac{\partial \bar{P}_0}{\partial Z} \frac{\partial \bar{P}_x}{\partial Z} + \bar{P}_0 \frac{\bar{P}_{x_{i,j+1}} + \bar{P}_{x_{i,j-1}}}{\partial Z^2} \right]$

D1= $-3\left(\frac{R}{c}\right) \left[\left(\frac{\partial \bar{P}_0}{\partial \theta} \right)^2 \bar{h}^2 \cos\theta + 2\bar{h}\bar{P} \frac{\partial \bar{P}_0}{\partial \theta} \frac{\partial \bar{h}}{\partial \theta} \cos\theta - \bar{P}_0 \bar{h}^2 \frac{\partial \bar{P}_0}{\partial \theta} \sin\theta + \bar{P}_0 \bar{h}^2 \frac{\partial^2 \bar{P}_0}{\partial Z^2} \cos\theta \right]$

E1= $-3\left(\frac{R}{c}\right)\left(\frac{R}{L}\right)^2 \cos\theta \left[\left(\frac{\partial \bar{P}_0}{\partial Z} \right)^2 \bar{h}^2 + \bar{P}_0 \bar{h}^2 \frac{\partial^2 \bar{P}_0}{\partial Z^2} \right] + \left(\frac{R}{c}\right) \left[\frac{\partial \bar{P}_0}{\partial \theta} \Lambda \cos\theta - \Lambda \bar{P}_0 \sin\theta + i2\Lambda' \bar{P}_0 \cos\theta \right]$

Along Y-direction

Calculation of P_y:

$$\bar{P}_{y_{i,j}} = \frac{B2 + C2 + D2 + E2}{A2} \qquad \text{..... (3.40)}$$

where A2= $\left[3\bar{h}^2 \frac{\partial \bar{h}}{\partial \theta} \frac{\partial \bar{P}_0}{\partial \theta} + \bar{h}^3 \frac{\partial^2 \bar{P}_0}{\partial \theta^2} + \left(\frac{R}{L}\right)^2 \bar{h}^3 \frac{\partial^2 \bar{P}_0}{\partial Z^2} - \bar{P}_0 \bar{h}^3 \left(\frac{2}{\Delta\theta^2} + \left(\frac{R}{L}\right)^2 \frac{2}{\Delta Z^2} \right) + \Lambda \frac{\partial \bar{h}}{\partial \theta} + i2\Lambda' \bar{h} \right]$

B2= $-\frac{\partial \bar{P}_y}{\partial \theta} \left[2 \frac{\partial \bar{P}_0}{\partial \theta} \bar{h}^3 + 3\bar{h}^2 \frac{\partial \bar{h}}{\partial \theta} \bar{P}_0 \right] - \bar{h}^3 \bar{P}_0 \frac{\bar{P}_{y_{i+1,j}} + \bar{P}_{y_{i-1,j}}}{\partial \theta^2} - \Lambda \bar{h} \frac{\partial \bar{P}_y}{\partial \theta}$

C2= $-\left(\frac{R}{L}\right)^2 \bar{h}^3 \left[2 \frac{\partial \bar{P}_0}{\partial Z} \frac{\partial \bar{P}_y}{\partial Z} + \bar{P}_0 \frac{\bar{P}_{y_{i,j+1}} + \bar{P}_{y_{i,j-1}}}{\partial Z^2} \right]$

D2= $-3\left(\frac{R}{c}\right) \left[\left(\frac{\partial \bar{P}_0}{\partial \theta} \right)^2 \bar{h}^2 \sin\theta + 2\bar{h}\bar{P} \frac{\partial \bar{P}_0}{\partial \theta} \frac{\partial \bar{h}}{\partial \theta} \sin\theta + \bar{P}_0 \bar{h}^2 \frac{\partial \bar{P}_0}{\partial \theta} cos\theta + \bar{P}_0 \bar{h}^2 \frac{\partial^2 \bar{P}_0}{\partial Z^2} \sin\theta \right]$

E2= $-3\left(\frac{R}{c}\right)\left(\frac{R}{L}\right)^2 \sin\theta \left[\left(\frac{\partial \bar{P}_0}{\partial Z} \right)^2 \bar{h}^2 + \bar{P}_0 \bar{h}^2 \frac{\partial^2 \bar{P}_0}{\partial Z^2} \right] + \left(\frac{R}{c}\right) \left[\frac{\partial \bar{P}_0}{\partial \theta} \Lambda \sin\theta + \Lambda \bar{P}_0 \cos\theta + i2\Lambda' \bar{P}_0 \sin\theta \right]$

Calculating the value of P_0, from equation (3.38), and applying in partial differential equation (3.39) and (3.40) the value of $P_{x_{i,j}}$ and $P_{y_{i,j}}$ can be calclated. Integrating it over the bearing pad surface we can find the values for the stiffness and damping parameters. In matrix form it can be expressed as:

$$K + i\omega B = \int_{-0.5}^{0.5} \int_{\xi}^{\xi+\alpha} \begin{pmatrix} P_x \cos\theta & P_x \sin\theta \\ P_y \cos\theta & P_y \sin\theta \end{pmatrix} R d\theta dz \qquad \text{.....} (3.41)$$

Where 'K' and 'B' are the dynamic stiffness and damping parameters.

The real part of the above matrix can be written as:

$$\left.\begin{matrix} K_{rr} \\ K_{\theta r} \end{matrix}\right\} = \int_{-L/2}^{L/2} \int_{\xi}^{\xi+\alpha} P_x \left\{\begin{matrix} \cos\theta \\ \sin\theta \end{matrix}\right\} R d\theta dz \qquad \left.\begin{matrix} K_{\theta\theta} \\ K_{r\theta} \end{matrix}\right\} = \int_{-L/2}^{L/2} \int_{\xi}^{\xi+\alpha} P_y \left\{\begin{matrix} \cos\theta \\ \sin\theta \end{matrix}\right\} R d\theta dz \quad \text{... (3.42)}$$

The imaginary part is:

$$\left.\begin{matrix} B_{rr} \\ B_{\theta r} \end{matrix}\right\} = \frac{1}{\omega} \int_{-L/2}^{L/2} \int_{\xi}^{\xi+\alpha} P_x \left\{\begin{matrix} \cos\theta \\ \sin\theta \end{matrix}\right\} R d\theta dz \qquad \left.\begin{matrix} B_{\theta\theta} \\ B_{r\theta} \end{matrix}\right\} = \frac{1}{\omega} \int_{-L/2}^{L/2} \int_{\xi}^{\xi+\alpha} P_y \left\{\begin{matrix} \cos\theta \\ \sin\theta \end{matrix}\right\} R d\theta dz \quad \text{... (3.43)}$$

The non-dimensional form of dynamic coefficients can be expressed as

$$\begin{aligned} \bar{K}_{rr}, \bar{K}_{r\theta}, \bar{K}_{\theta r}, \bar{K}_{\theta\theta} &= \frac{cK_{rr}}{W}, \frac{cK_{r\theta}}{W}, \frac{cK_{\theta r}}{W}, \frac{cK_{\theta\theta}}{W} \\ \bar{B}_{rr}, \bar{B}_{r\theta}, \bar{B}_{\theta r}, \bar{B}_{\theta\theta} &= \frac{cB_{rr}\omega}{W}, \frac{cB_{r\theta}\omega}{W}, \frac{cB_{\theta r}\omega}{W}, \frac{cB_{\theta\theta}\omega}{W} \end{aligned} \qquad \text{..... (3.44)}$$

3.3 Flow Chart

A brief and step by step description to find out different static parameters like front face and back face pad pressure, load carrying capacity and dynamic characteristics of stiffness and damping for the pivotless tilting pad gas journal bearing using MATLAB code given below.

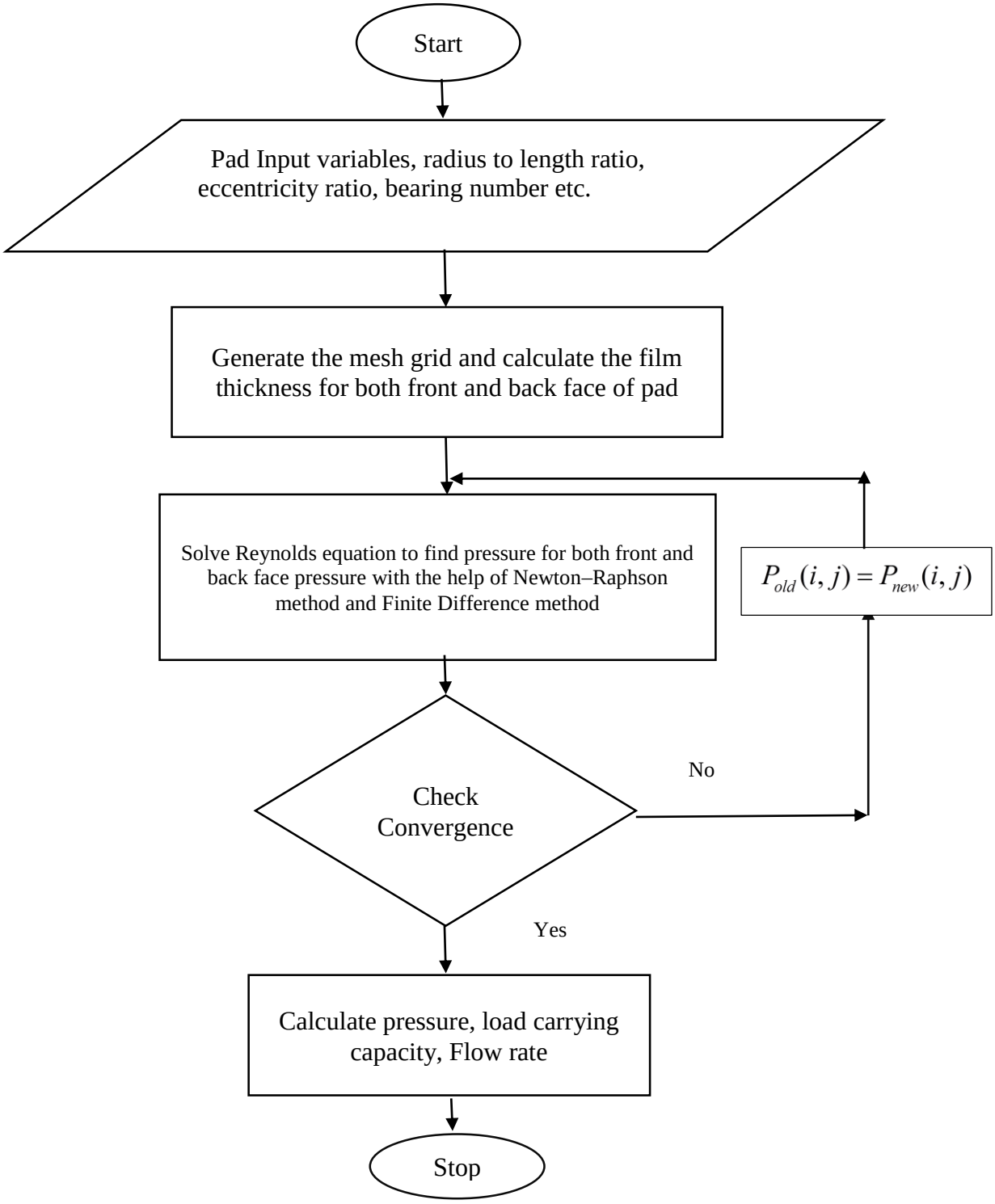

Flow chart to evaluate dynamic parameters of stiffness and damping is given below.

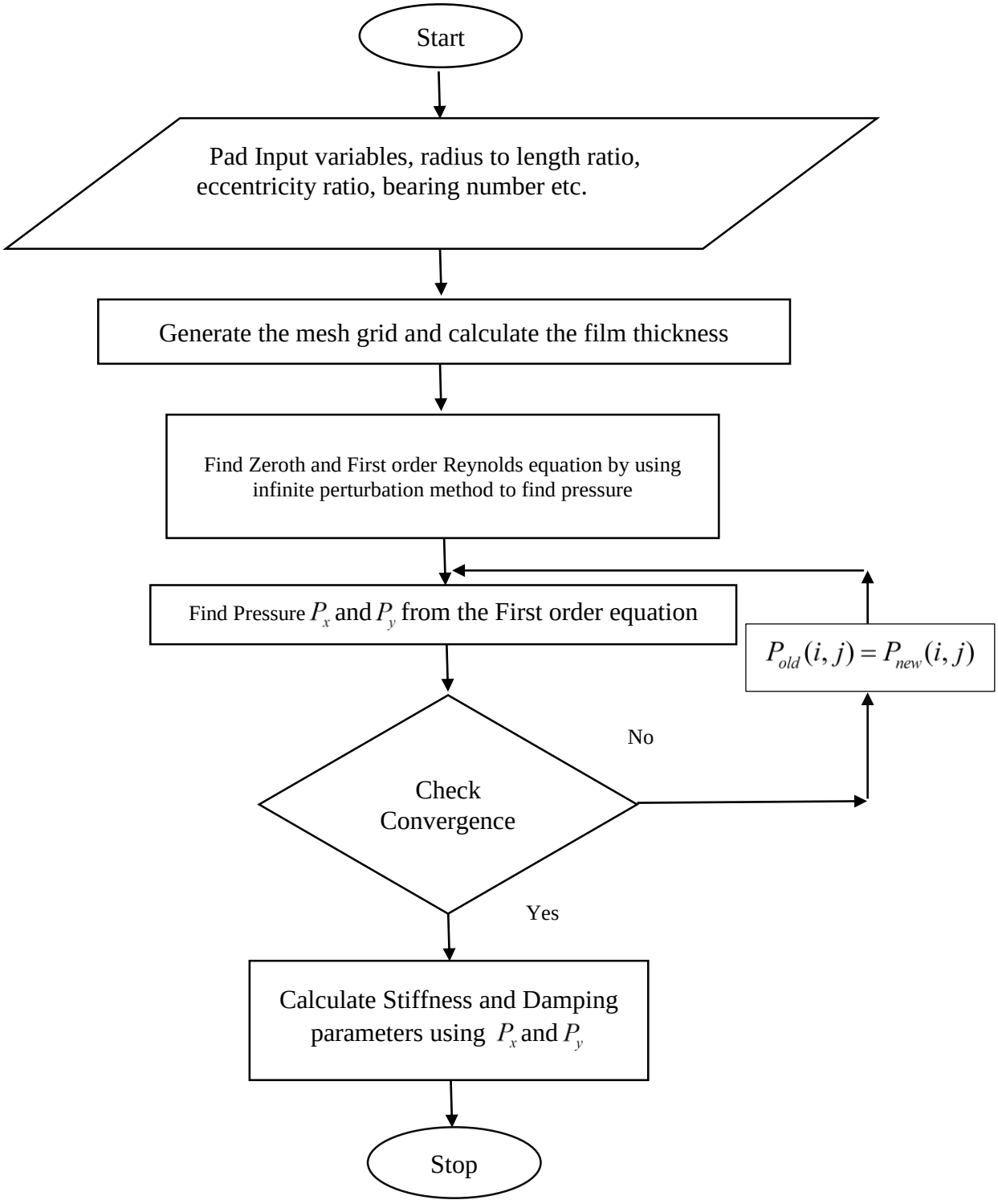

4. Results and Discussion CHAPTER 4

Current research is an effort to understand the behavior of performance parameter of pivot less tilting pad gas journal bearing by analyzing it theoretically and graphically. This paper focused on evaluating the method to calculate dymnamic parameters for stiffness and damping behaviour of a gas journal bearing system. It also explains the static parameters of pad front and back pressure, variation of load carrying capacity with respect to different parameters like angle ratio, eccentricity ratio, film thickness, and bearing number, frictional shear stress and coefficent of friction parameters . Converging –diverging films often give rise to instabilities; hence the simulation curves presented here are only validated for true convergent aerodynamic films.

4.1 Pressure Profile

Because of the shearing action between fluid and pad front surface there is a pressure comes into the picture. This pressure can be calculated by using the Reynolds equation. Using MATLAB and finite difference method pressure profile can be found out.

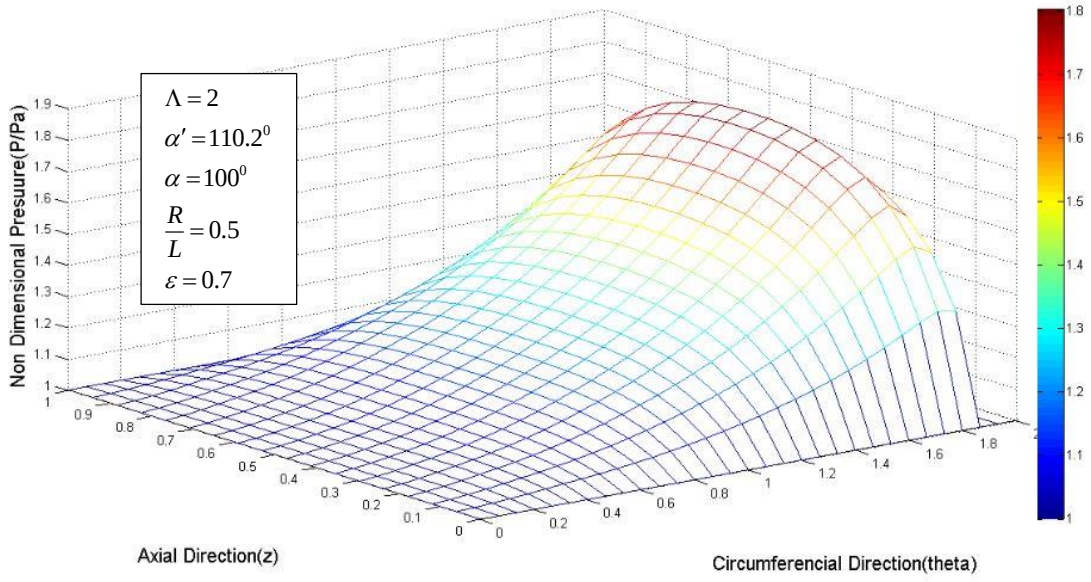

(Fig-4.1: 3-D Non-dimensional pressure distribution at the front face)

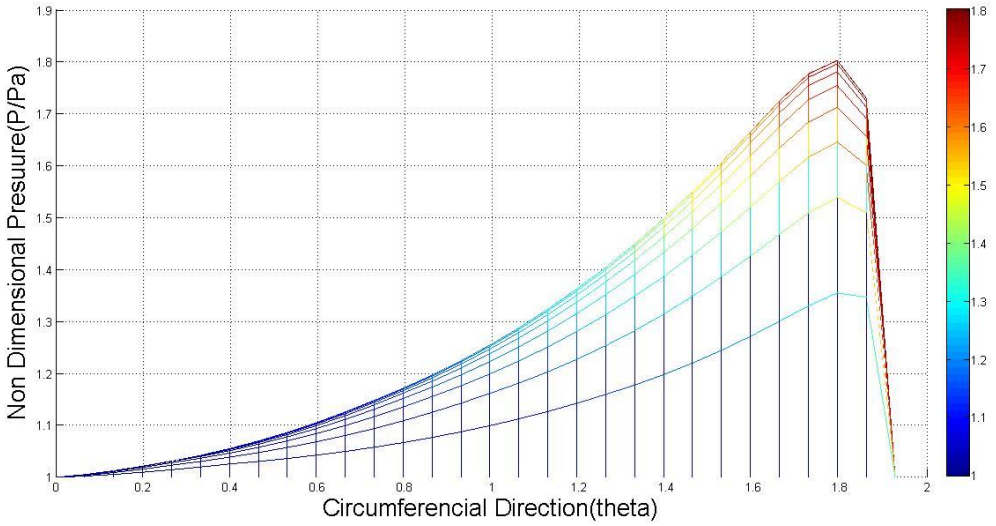

(Fig-4.2: Non-dimensional pressure distribution on the pad surface along circumferential direction)

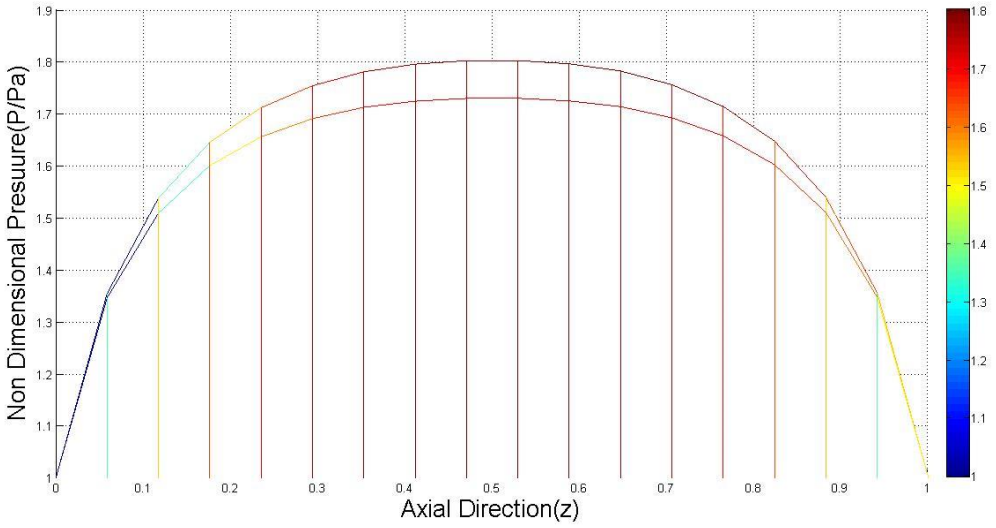

(Fig-4.3: Non-dimensional Pressure distribution on the pad surface along axial

The result that we are getting for the pressure profile is only for the single pad. For a particular value of eccentricity ratio and fixed input parameters the pressure profile increases towards the converging medium. At the edge of the pad, pressure is atmospheric.

To calculate the total pressure we need, to sum up, the effect of individual pad pressure, as each pad acts separately over the bearing surface.

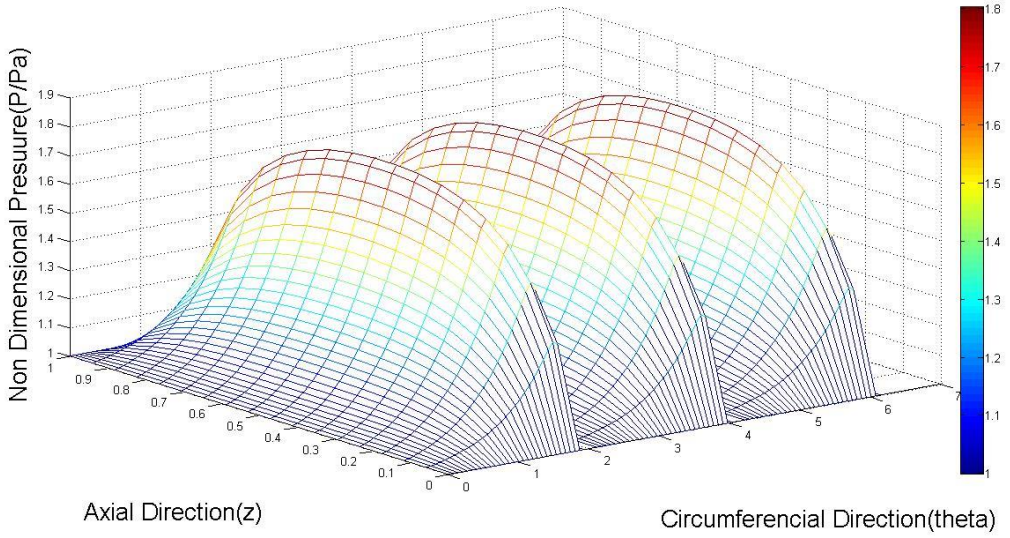

(Fig-4.4: 3-D Non-dimensional total pad pressure distribution at the front face)

4.2 Back Pad Pressure

Gas from the front face passes to the back face through the network of holes creating a pressure at the back face which completely eliminates the need of pivot at the back face of the pad. This pressure helps for positioning the pad. Back pad pressure can be calculated by using the equation (3.26).

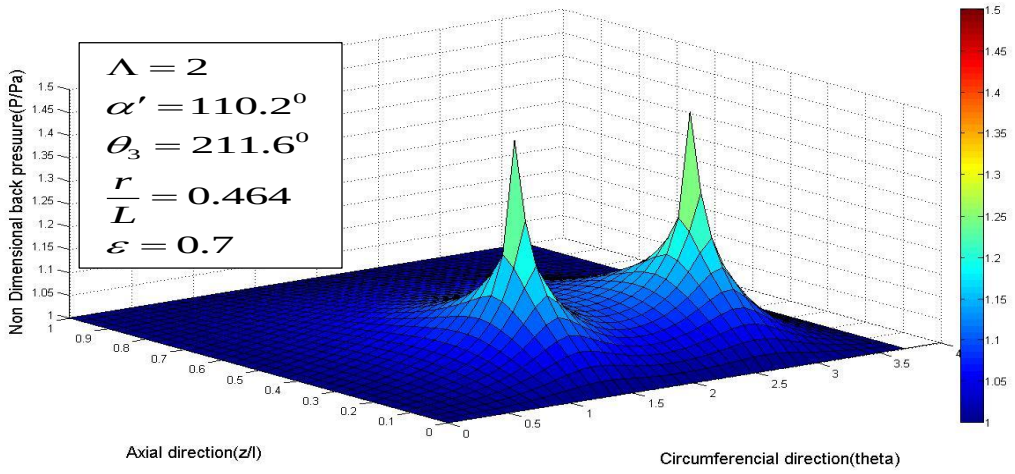

(Fig-4.5: 3-D Non-dimensional Pressure distribution at the back face of pad)

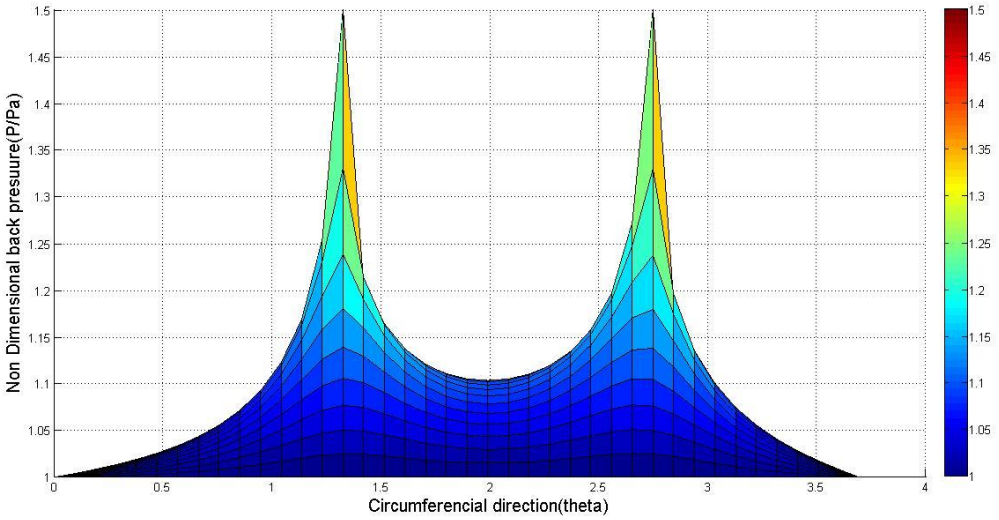

(Fig-4.6: Non-dimensional Back pressure distribution on the pad surface along circumferential direction)

Because of the symmetry only one-half of the back face is shown. As there are two connecting holes are present in one-half so two stiff points are coming into the picture. The pressure at the bleed hole and connecting holes can be taken as same, which is slightly greater than the atmospheric pressure.

4.3 Load carrying capacity

Load carrying capacity depends upon various facors like pad front face pressure, wedge given at trailing edge, angle ratio, eccentricity ratio, dynamic viscosity of fluid, etc. So, by changing parameters we can adjust load carrying capacity of a bearing. In equation, (3.20) expression for non-dimensional load carrying capacity is shown. Where $\overline{W_r}$ and $\overline{W_t}$ are non-dimensional load carrying capacity along and normal to the maximum film thickness direction.

4.3.1 Load carrying capacity Vs. Eccentricity ratio

Eccentricity ratio is the ratio between eccentricity and radial clearance of the journal bearing. It can be adjusted by changing the radius of the journal as per the convenience. Eccentricity ratio can maximum varies from 0 to1. The relation between load carrying capacity and eccentricity ratio given below.

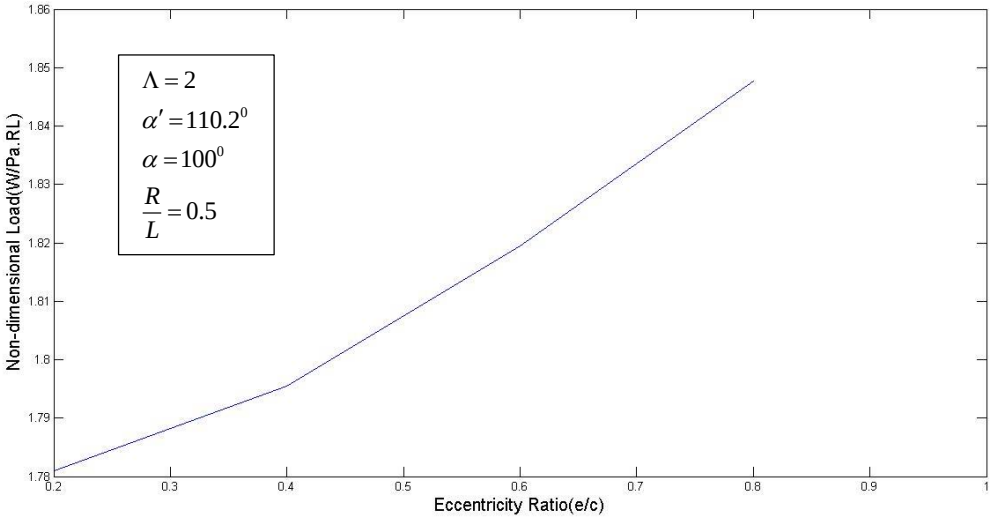

(Fig 4.7: Variation of Non-dimensional pad load with eccentricity ratio)

As eccentricity ratio increases, the eccentricity will increase. Increasing value of eccentricity is caused to squeeze out more amount of fluid by increasing the fluid pressure that helps to increase the load carrying capacity.

4.3.2 Load carrying capacity Vs. Pad Angle

In case of tilting pad journal bearing as pad angle increases starting from leading edge, gap between pad and journal known as film thickness is also increases. Film thickness is one of the most important parameters that will affect the load carrying capacity. Load carrying capacity has the direct influence on the fluid film thickness as more is the load carrying capacity more is the amount of fluid that is squeezed out. So as we go on increasing the pad angle, load carrying capacity increases.

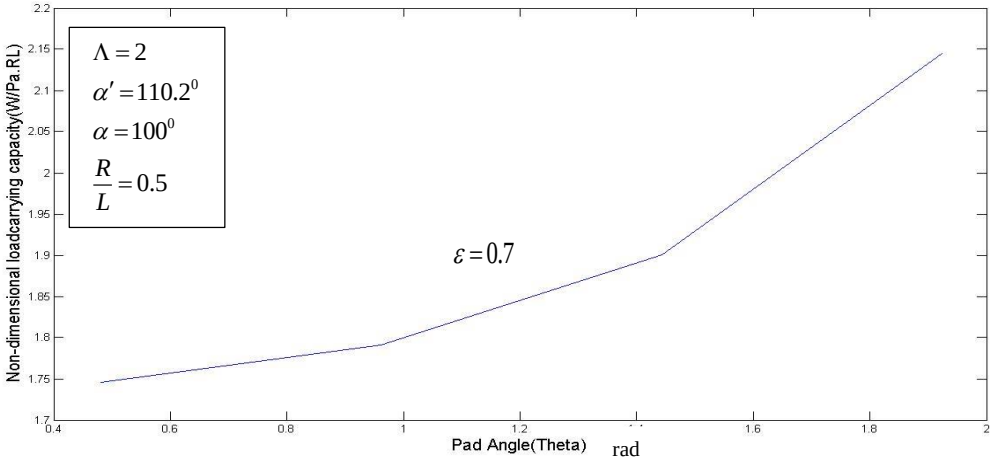

(Fig-4.8: Variation of Non-dimensional pad load capacity with pad angle)

4.3.3 Load carrying capacity Vs. Film Thickness ratio

Film thickness ratio is the ratio between film thickness and radial clearance. As the load carrying capacity will decrease the gap between the pad and journal will increase. Resulting increasing in the film thickness ratio. This can explained well by the graph below.

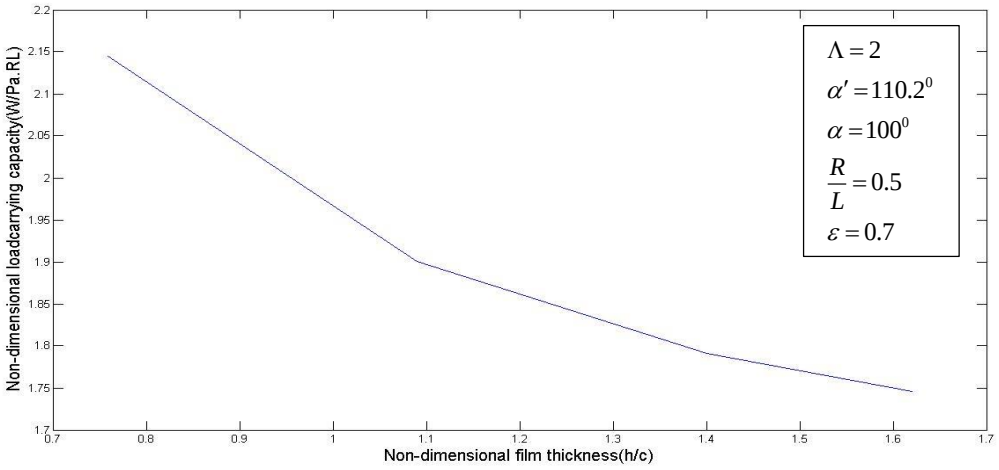

(Fig-4.9: Variation of Non-dimensional pad load capacity with film thickness ratio)

4.3.4 Load carrying capacity Vs. Bearing number

Bearing number is a non-dimensional term that denoted as ' Λ ' and expressed as $\Lambda = \frac{6\mu\omega}{P_a}\left(\frac{R}{C}\right)^2$. The bearing number can be varied by varying different parameters like the radius of journal, speed of rotation or by using different gases having different dynamic viscosity.

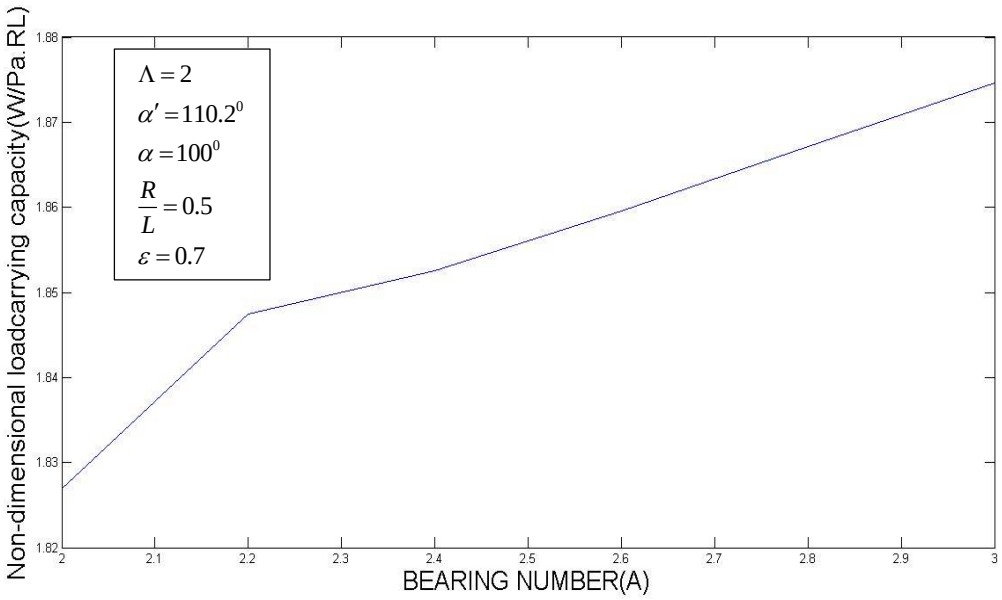

(Fig-4.10: Variation of Non-dimensional pad load capacity with bearing number)

Higher the viscosity of fluid higher will be the load carrying capacity as fluid will behave stiffer than a lower viscosity fluid. Similarly when we increase the speed of rotation in a self-acting bearing, more pressure will generate in the converging medium resulting increase in load carrying capacity. As we go on increase, the bearing number after certain value the increase in value of load carrying capacity is not up to the mark. There are also certain design limitations beyond which we cannot increase the bearing number for example if we go on increasing the speed because of whirling the shaft may fail.

4.3.5 Frictional Force Vs. Eccentricity Ratio

Increase in eccentricity ratio will result in increase in load carrying capacity. Because of the shearing action of fluid, frictional force comes in to play.

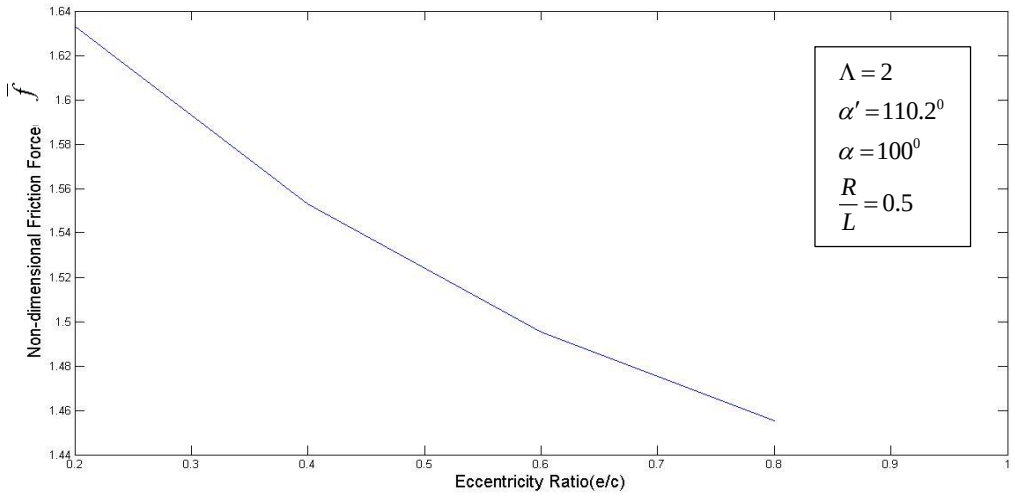

(Fig-4.11: Variation of Non-dimensional frictional force with eccentricity Ratio)

4.3.6 Coefficient of friction Vs. Eccentricity Ratio

As eccentricity ratio increases load carrying capacity also increases, resulting decrease in the coefficient of friction.

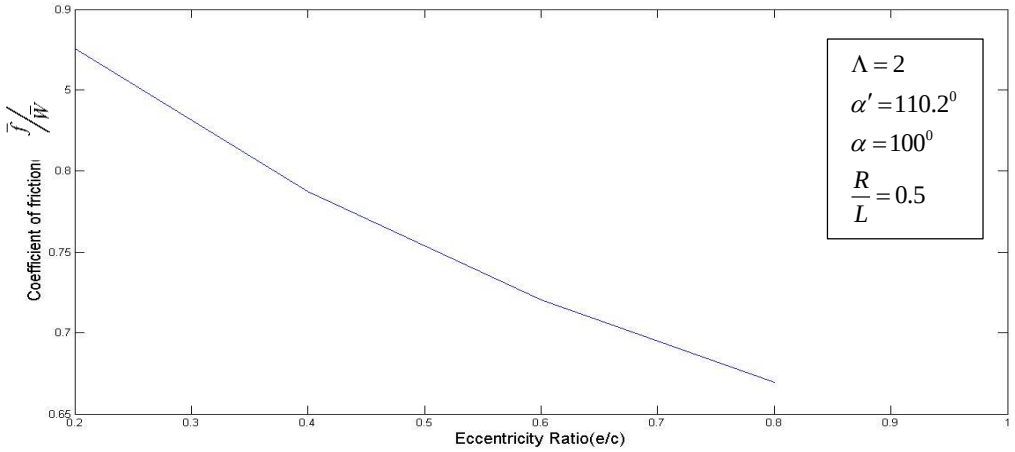

(Fig-4.12: Variation of coefficient of friction with eccentricity Ratio)

4.3.7 Film thickness Ratio Vs. Eccentricity Ratio

For a perticular value of θ, the result between the film thickness ratio and eccentricity ratio is shown below.

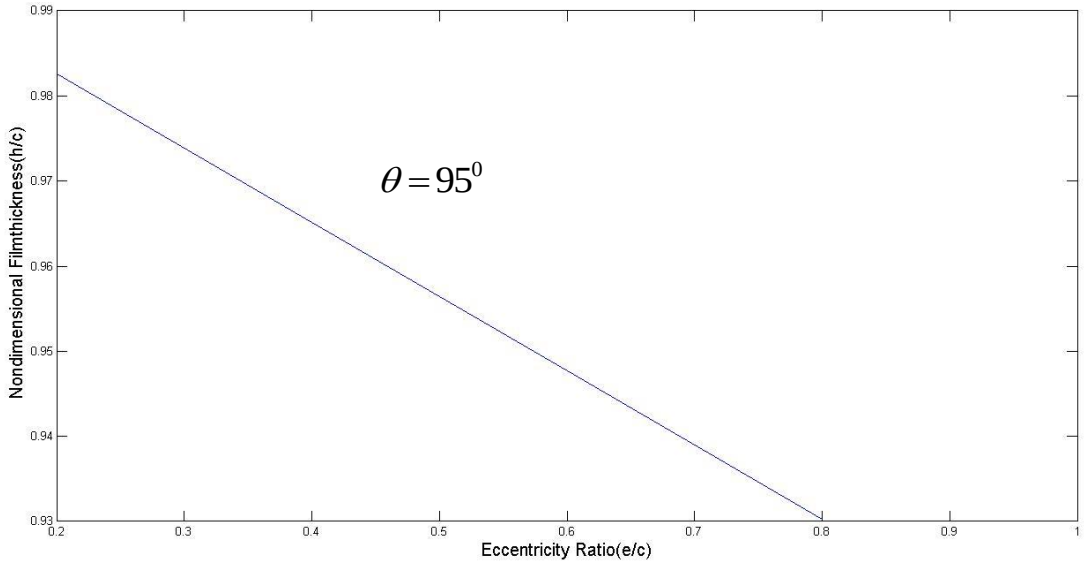

(Fig-4.13: Variation of Non-dimensional film thickness ratio with eccentricity Ratio)

5. Conclusion CHAPTER 5

Current research on aerodynamic analysis of pivot less tilting pad journal bearing was an attempt to study feasibility of using in high speed small turbo expander and turbocharger. Converging-diverging films often give rise to instabilities, hence simulation curves presented here are truly valid for convergent aerodynamic films.

- Non-dimensional pressure profile for tilting pad gas journal bearing was found in considerable range shown in the figure (4.1) and (4.2).
- Considering the static equilibrium condition non-dimensional back pad pressure is calculated as shown in figure (4.3) and is found sufficient for positioning the pad.
- Load carrying capacity can be changed by varying the bearing number which is a function of dynamic viscosity, speed of operation, radial clearance etc. figure (4.10) shows the relation between load carrying capacity and bearing number. As bearing number increases non-dimensional load carrying capacity is also increases.
- The graph between non-dimensional load carrying capacity and eccentricity ratio is plotted in figure (4.4). As eccentricity ratio increases pad load capacity is also increased.
- Load carrying capacity and pressure profiles shows best results when eccentricity ratio is above 0.7.
- Increasing the pad angle starting from leading edge, we get a converging medium which results in increasing the value of load carrying capacity for a constant eccentricity ratio. The relation is shown in the figure (4.8).
- Keeping the film thickness as a constant, if we go on increasing the value of eccentricity ratio the load carrying capacity is also increases.

- The relation between co-efficient of frictional force with respect to eccentricity ratio is shown in the figure (4.12), where coefficient of friction steadily decreases with respect to eccentricity ratio.
- The relation between non-dimensional film thickness and eccentricity ratio for a particular value of $\theta = 95^0$ is shown in figure (4.13).

Future Scopes:

- By balancing all the forces, the equilibrium position of the shaft can be found out.
- Pad geometry and pad material behaviour can also be studied for further enhancement in characteristics of pivot less tilting pad gas bearing.
- Experimental set up is required to check the mathematical model.
- Dynamic characteristics like direct and cross coupled stiffness and damping parameters of the pad can be calculated.

References

1. ***Ghosal Arindam***, "A Review of Fluid Film Bearing", Proceedings of the Asian Congress of Fluid Mechanics, 2010.
2. ***Bhandari V B***, "Design of Machine Elements", pp-564-644, 2013.
3. ***Timothy Dimond et al.*** "A Review of Tilting Pad Bearing Theory", Article Id 908469, International Journal Rotating MachineryVolume 2011.
4. ***Chakrabarty Anindya***, "Analytical and Experimental studies of gas bearing for cryogenic turbo-expander", 2000, PP 93-114.
5. ***O. Reynolds***,"on the Theory of lubrication and its application to Mr. Beauchamp Tower's experiments, including an experimental determination of viscosity of olive oil," Philosophical Transactions of the Royal Society, vol.177,pp 157-234, 1886.
6. **Ghosh S, Mukherjee P, Sarangi S.** Development of bearings for a small high-speed cryogenic turbo expander. Industrial Lubrication and Tribology2012; 64(1):3-10.
7. **A. *Sommerfeld***, "Zur Hydrodynamicsche Theory der Schiermittelrebung", Zeitschrift ur Mathematics and Physik vol 50, pp97-155, 1904.
8. ***J.K. Lund***,"Spring and damping coefficients for the tilting pad journal bearing", ASLE Transactions, vol.42, no.4, pp 342-352, 1964.
9. ***Schmidt, C.*** Gas Bearing Turboexpanders for Cryogenic plants, Paper B1, 6th International Gas Bearing Symposium, University of Southampton (1974).
10. ***M.K. Ghosh, B.C. Majumdar, Mihir Sarangi***, (2013)"Theory of Lubrication", Tata McGraw-Hill, New Delhi.
11. ***Huang, Ping***, "Numerical Calculation of Lubrication (2013)", Wiley Publication, Singapore.

12. ***J.C. Nicholas, E.J.Gunter, P.E. Allaire***, "Stiffness and Damping Coefficients for the Five Pad Tilting Pad Bearing", ASLE/ASME Lubrication Conference, Kanas City, Missourl, October 3-5,1977
13. ***Dong-Jin Park et al***., "Theoritical considerations of static and dynamic characteristics of air foil thrust bearing with tilt and slip flow", Republic of Korea, October,2007.
14. ***G.Pitts***, "A design method for Tilting-Pad gas journal bearings", Department of Mechanical Engineering, 'the University of Southampton, England, 1970.
15. ***Uucel Yucel***,"Calcukation of Dynamic Coefficients for Fluid Film Journal Bearing", Department of Mathematics, Pamukkale University, Denizli, 2004.
16. ***Agrawal Giri L***.,"Foil air/gas Bearing Technology-An Overview", ASME International Gas Turbine and Aeroengine Congress and exhibition, Orlando, Florida, 1997.
17. ***Yu Hou et al***,"Numerical analysis on the static performance of Tilting Pad gas Journal Bearing in subsystems", Tribology International,2013,pp-70-79.
18. ***Richard K. Niffin,***"Development of an Analytical Design Tool for Journal Bearings", August 2009, pp-8-30.
19. ***Gwidon W. Stachowiak, Andrew W. Batchlor,***"Engineering Tribology", Butterworth Heinemann publication, Australia,pp-201-279.
20. ***Stefano Morosi,***"From Hybrid to Actively-Controlled Gas Lubricated Bearings-Theory and Experiment"(2011), Dnamark,pp-63-84.